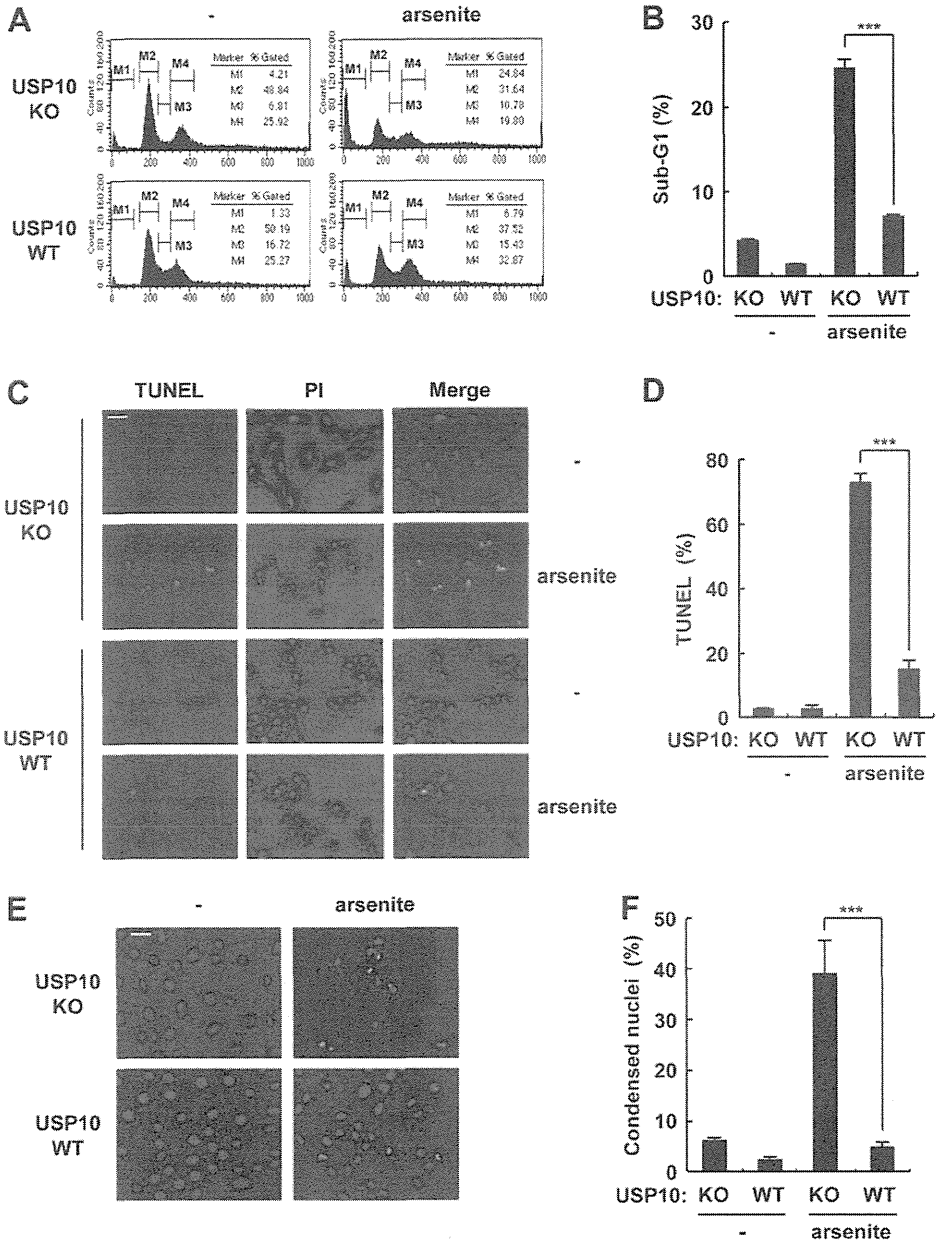

FIG 7 Genetic ablation of USP10 enhances arsenite-induced apoptosis. (A) *USP10*$^{\Delta/\Delta}$ (KO) and *USP10*$^{+/+}$ (WT) MEFs were treated with 1 mM sodium arsenite for 60 min, washed, and further cultured in fresh medium for 10 h. MEFs were stained with propidium iodide (PI), and the sub-G_1 apoptotic population was analyzed by flow cytometry. (B) Proportion of the sub-G_1 fraction in *USP10*$^{\Delta/\Delta}$ (KO) and *USP10*$^{+/+}$ (WT) MEFs. (C to F) Apoptotic cells were also assessed by a TUNEL assay (C and D) or staining of nuclei with Hoechst 33258 (E and F) under a fluorescence microscope. In all panels, the values denote the means ± SD. ***, $P < 0.001$. The bars indicate 50 μm.

mUSP10^{C418A} rescued all three activities, although their activities to SGs and apoptosis were slightly less than those of mUSP10^{WT} (Fig. 10E and F). These results indicate that the PABP1 binding and deubiquitinase activity of USP10 are dispensable for these three SG-associated activities. On the other hand, mUSP10$^{77–792}$, mUSP10$^{95–792}$, and mUSP10$^{1–114}$ barely rescued any activities in *USP10*$^{\Delta/\Delta}$ MEFs, thus indicating that both N-terminal and C-terminal regions of mUSP10 are required for these three activities (Fig. 10E and F). Interestingly, the expression of mUSP10$^{1–114}$ or mUSP10$^{95–792}$ in *USP10*$^{\Delta/\Delta}$ MEFs augmented arsenite-induced ROS production (Fig. 10F), thus indicating that these mutants might interact with the proteins negatively controlling ROS production. In this respect, mUSP10$^{1–114}$ might augment the arsenite-induced ROS production in *USP10*$^{\Delta/\Delta}$ MEFs through the interaction with G3BP1, since mUSP10$^{1–114}$ can interact with G3BP1 (Fig. 2C). In addition, it should be noted that arsenite-induced ROS production and apoptosis in the *USP10*$^{\Delta/\Delta}$ MEFs expressing USP10 mutants were correlated qualitatively but not

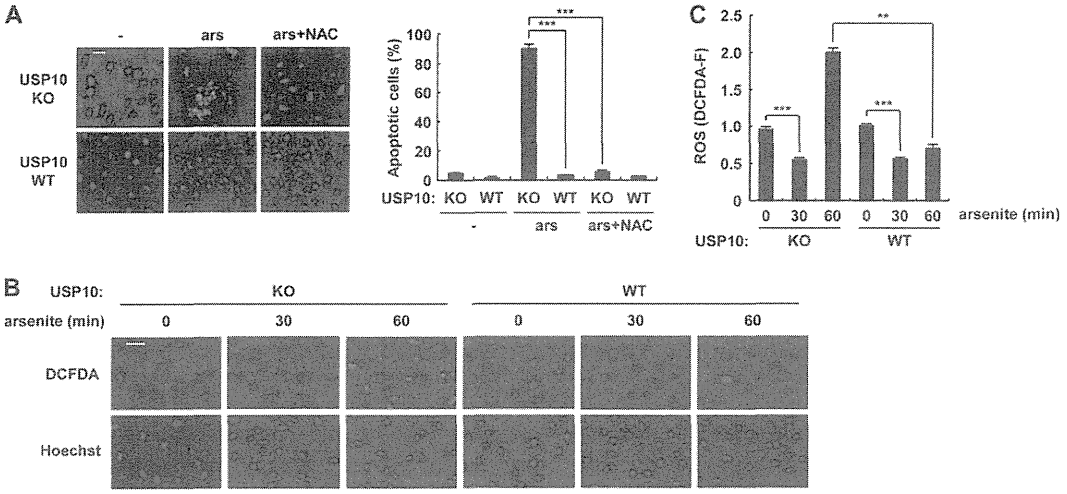

FIG 8 USP10 plays critical roles in ROS production and ROS-dependent apoptosis. (A) *USP10*$^{\Delta/\Delta}$ (KO) and *USP10*$^{+/+}$ (WT) MEFs were pretreated with or without 5 mM *N*-acetylcysteine (NAC) and further treated with 1 mM sodium arsenite (ars) for 60 min. The cells were washed, cultured in fresh medium for 10 h, and then stained with Hoechst 33258. The numbers of cells containing condensed nuclei (apoptotic cells) were counted by a fluorescence microscope. The bar indicates 50 μm. (B and C) *USP10*$^{\Delta/\Delta}$ (KO) and *USP10*$^{+/+}$ (WT) MEFs were treated with 1 mM sodium arsenite for 0, 30, and 60 min and stained with 5 μM CM-H_2DCFDA (a redox-sensitive dye) (green) and Hoechst 33258 (blue) for 5 min at 37°C. The staining of the cells was characterized under a fluorescence microscope (B). The bar indicates 50 μm. ROS levels (DCFDA-F) were quantitatively determined by the fluorescence analysis software (C). In all panels, the values denote the means ± SD. **, $P < 0.01$; ***, $P < 0.001$.

precisely quantitatively (Fig. 10E and F). We measured the ROS production and apoptosis in these MEFs 100 min and 4 h after arsenite treatment, respectively. The difference between the two assays might explain why ROS production and apoptosis in MEFs do not quantitatively show an exact correlation.

Two different mechanisms of the arsenite-induced ROS reduction were considered: ROS reduction is specific to arsenite treatment, or the reduction is a common function of SGs. To distinguish which of these two possibilities was the case, we attempted to induce SGs without arsenite treatment (5). The expression of exogenous G3BP1 without arsenite treatment successfully induced SGs in 293T cells, and it reduced the ROS level only in the cells with SGs (Fig. 11A). All three N-terminal deletion mutants of G3BP1 that lost the ability to induce SGs simultaneously failed to suppress ROS production (Fig. 11B and C). These three inactive G3BP1 mutants did not interact with USP10 in 293T cells (27). Since SGs induced by exogenous G3BP1 collected G3BP1 into SGs and reduced the amount of G3BP1 outside SGs (Fig. 11D), exogenous G3BP1-induced SGs contained endogenous G3BP1. In addition to arsenite, we observed an ROS reduction in 293T cells exposed to heat shock, and the reduction was detected simultaneously with SG formation (Fig. 12). Collectively, these results indicate that G3BP1-induced SGs can reduce the ROS level and that this effect is not specific for exposure to arsenite.

Treatment of cells with a protein synthesis inhibitor, cycloheximide (CHX), has been shown to prevent SG formation (20) (Fig. 13A and B). We next examined whether CHX treatment prevents arsenite-induced ROS reduction. Pretreatment of 293T cells with CHX upregulated the ROS level under steady-state conditions (Fig. 13C), suggesting that ongoing protein synthesis is required for downregulation of the steady-state ROS level. Upon treatment with arsenite, the ROS level was reduced, even in the CHX-treated

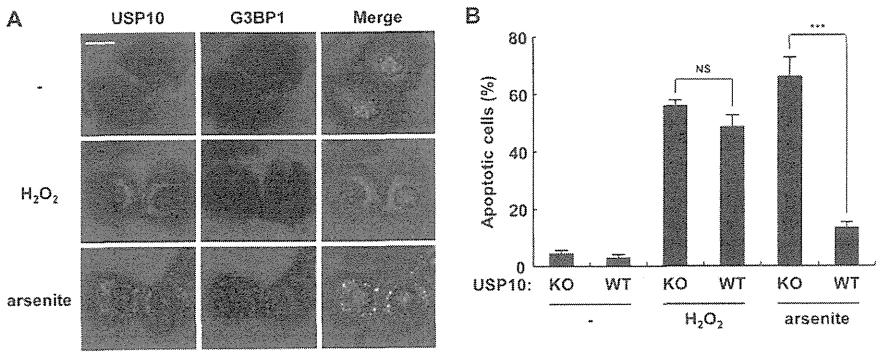

FIG 9 Hydrogen peroxide (H_2O_2) equivalently induces apoptosis in *USP10*$^{\Delta/\Delta}$ and *USP10*$^{+/+}$ MEFs. (A) *USP10*$^{+/+}$ MEFs were treated with 1 mM H_2O_2 for 60 min or 1 mM sodium arsenite for 60 min, fixed, and stained with anti-USP10-163 (green) and G3BP1 (red) antibodies. Nuclei were counterstained using Hoechst 33258 (blue). The staining of cells was examined by a fluorescence microscope. The bar indicates 20 μm. (B) *USP10*$^{\Delta/\Delta}$ (KO) and *USP10*$^{+/+}$ (WT) MEFs were treated with 1 mM H_2O_2 for 180 min or 1 mM sodium arsenite for 90 min, fixed, and stained with Hoechst 33258. The numbers of cells with condensed nuclei were counted using a fluorescence microscope. The values denote the means ± SD. ***, $P < 0.001$; NS, not significant.

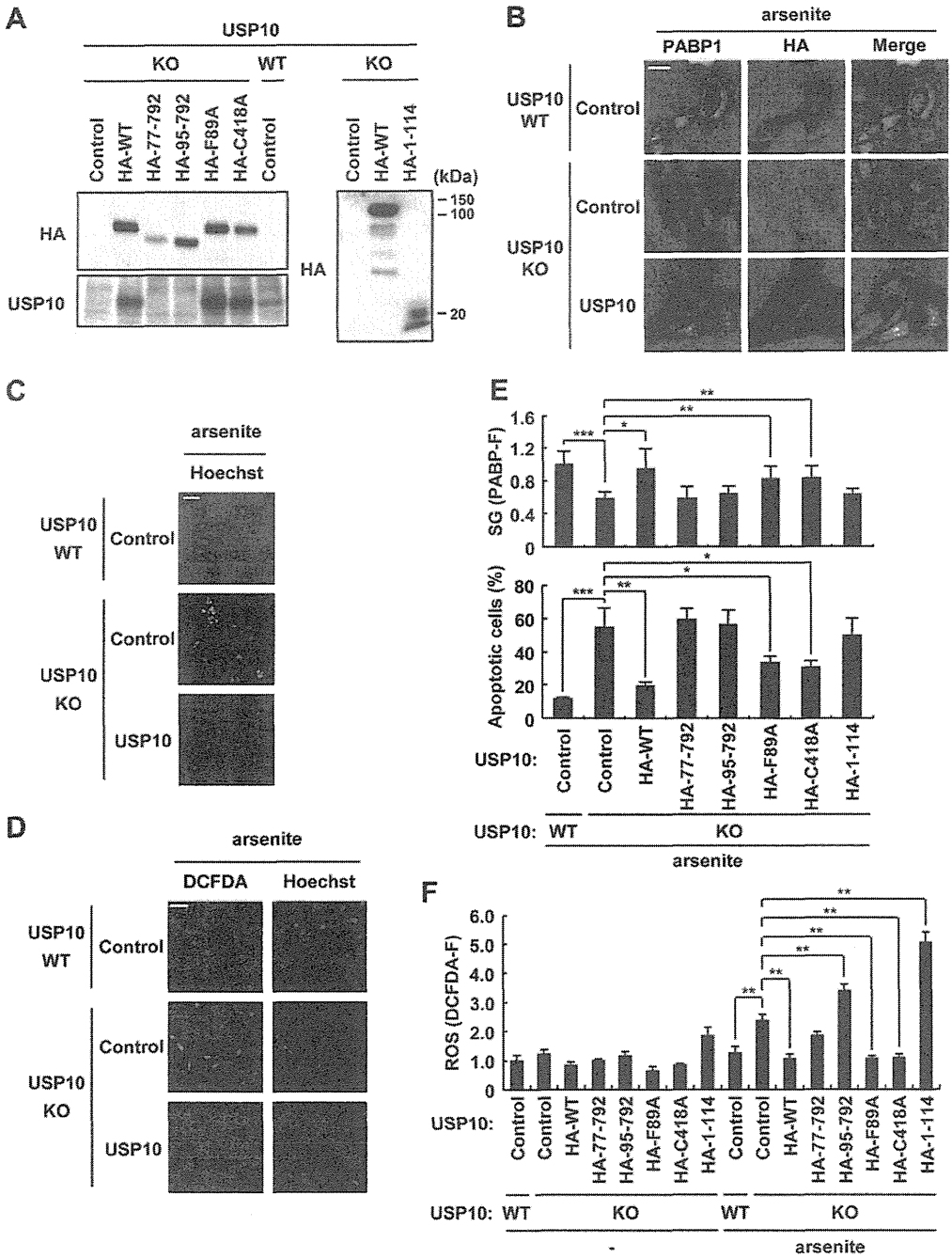

FIG 10 Domains of USP10 required for SG-associated functions. (A) *USP10*$^{\Delta/\Delta}$ (KO) and *USP10*$^{+/+}$ (WT) MEFs expressing a series of HA-mUSP10 mutants were established. The cell lysates were prepared from these transfectants and characterized using a Western blot analysis with anti-HA and anti-USP10-N antibodies. (B) Indicated MEFs were treated with 1 mM sodium arsenite for 60 min, and cells were stained with anti-PABP1 (green) and anti-HA (red) antibodies and Hoechst 33258 (blue). The bar indicates 20 μm. (C) Indicated MEFs were treated with 1 mM sodium arsenite for 100 min. The cells were washed and cultured in fresh medium for 4 h. The cells were then fixed and stained with Hoechst 33258 to detect apoptotic cells. The bar indicates 50 μm. (D) Indicated MEFs were treated with 1 mM sodium arsenite for 100 min and stained with 5 μM CM-H_2DCFDA (green) and Hoechst 33258 (blue) for 5 min at 37°C. The bar indicates 50 μm. (E) *USP10*$^{\Delta/\Delta}$ (KO) and *USP10*$^{+/+}$ (WT) MEFs expressing the indicated mUSP10 mutants were treated with 1 mM sodium arsenite and stained in a manner similar to that described for panel B. Upper panel, SG formation (PABP-F) was determined. MEFs were also treated with 1 mM sodium arsenite and stained in a manner similar to that described for panel C. Lower panel, the numbers of cells containing condensed nuclei were counted. (F) *USP10*$^{\Delta/\Delta}$ (KO) and *USP10*$^{+/+}$ (WT) MEFs expressing the indicated mUSP10 mutants were treated with 1 mM sodium arsenite and stained in a manner similar to that described for panel D. The ROS level (DCFDA-F) was measured. In all panels, the values denote the means ± SD. *, $P < 0.05$; **, $P < 0.01$; ***, $P < 0.001$.

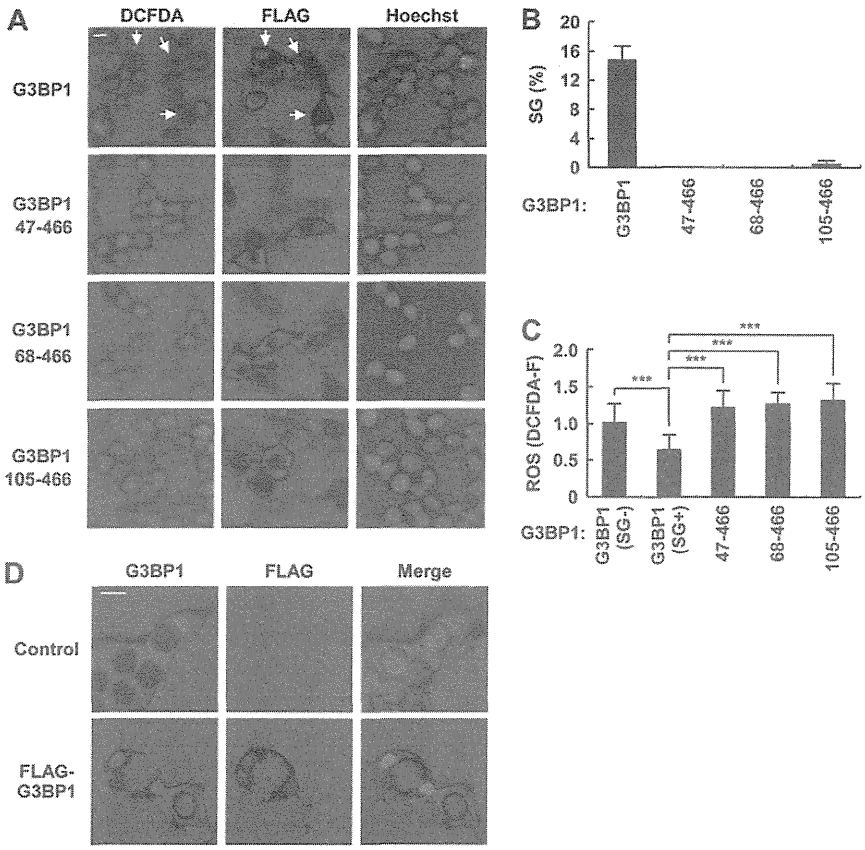

FIG 11 G3BP1-induced SGs reduce ROS production. (A to C) 293T cells were transfected with plasmids encoding FLAG-G3BP1^{WT} or the indicated deletion mutants (G3BP1$^{47-466}$, G3BP1$^{68-466}$, and G3BP1$^{105-466}$). The transfected cells were treated with 5 μM CM-H_2DCFDA (green) for 5 min at 37°C. The cells were then fixed and stained using anti-FLAG (red) and Hoechst 33258 (blue). (A) The arrows indicate SG-positive cells, and the bar indicates 10 μm. (B) SG percentages in cells stained with anti-FLAG. (C) ROS level (DCFDA-F) in FLAG-positive cells. (D) 293T cells were transfected with plasmid encoding FLAG-G3BP1^{WT}, fixed, and stained using anti-G3BP1 (green), anti-FLAG (red), and Hoechst 33258 (blue). The bar indicates 10 μm. In all panels, the values denote the means ± SD. ***, $P < 0.001$.

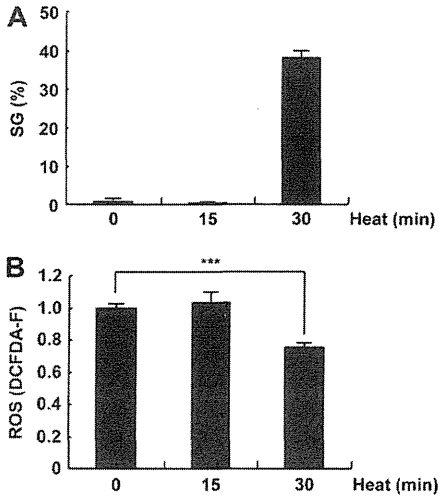

FIG 12 Heat shock reduces ROS production. (A and B) 293T cells were exposed to heat shock at 44°C for 0, 15, and 30 min. The SG percentages (A) and ROS levels (DCFDA-F) (B) are shown. The values denote the means ± SD. ***, $P < 0.001$.

cells; however, the reduction was less than that observed in the CHX-untreated cells (Fig. 13C). These results suggest that arsenite reduces the ROS level in both SG-dependent and SG-independent manners.

G3BP1 inhibits the antioxidant role of USP10 under steady-state conditions. We next assessed the role of endogenous G3BP1 and USP10 in ROS production (Fig. 14A). Knockdown of endogenous G3BP1 by using siRNA reduced the steady-state ROS levels in all six cell lines tested (Fig. 14B). The cellular ROS level was also reduced by another siRNA targeting the 3′ untranslated region of *G3BP1* mRNA (Fig. 14C and D), and the reduction of the ROS was rescued by the expression of siRNA-resistant *G3BP1* (Fig. 14E and F). It should be noted that the expression of G3BP1 in G3BP1 knockdown cells induced SGs, but the amount of SGs was lower than that observed in wild-type 293T cells (our unpublished observations). On the other hand, while knockdown of USP10 in the G3BP1 knockdown cells enhanced the ROS level, knockdown of USP10 in the G3BP1-competent cells had minimal effects on ROS production (Fig. 14G and H). Furthermore, exogenous USP10 reduced ROS production only in the G3BP1 knockdown cells and not in the G3BP1-competent cells (Fig. 14I and J). Collectively, these data demonstrate that USP10 possesses an antioxidant activity; however, the activity observed under steady-state condi-

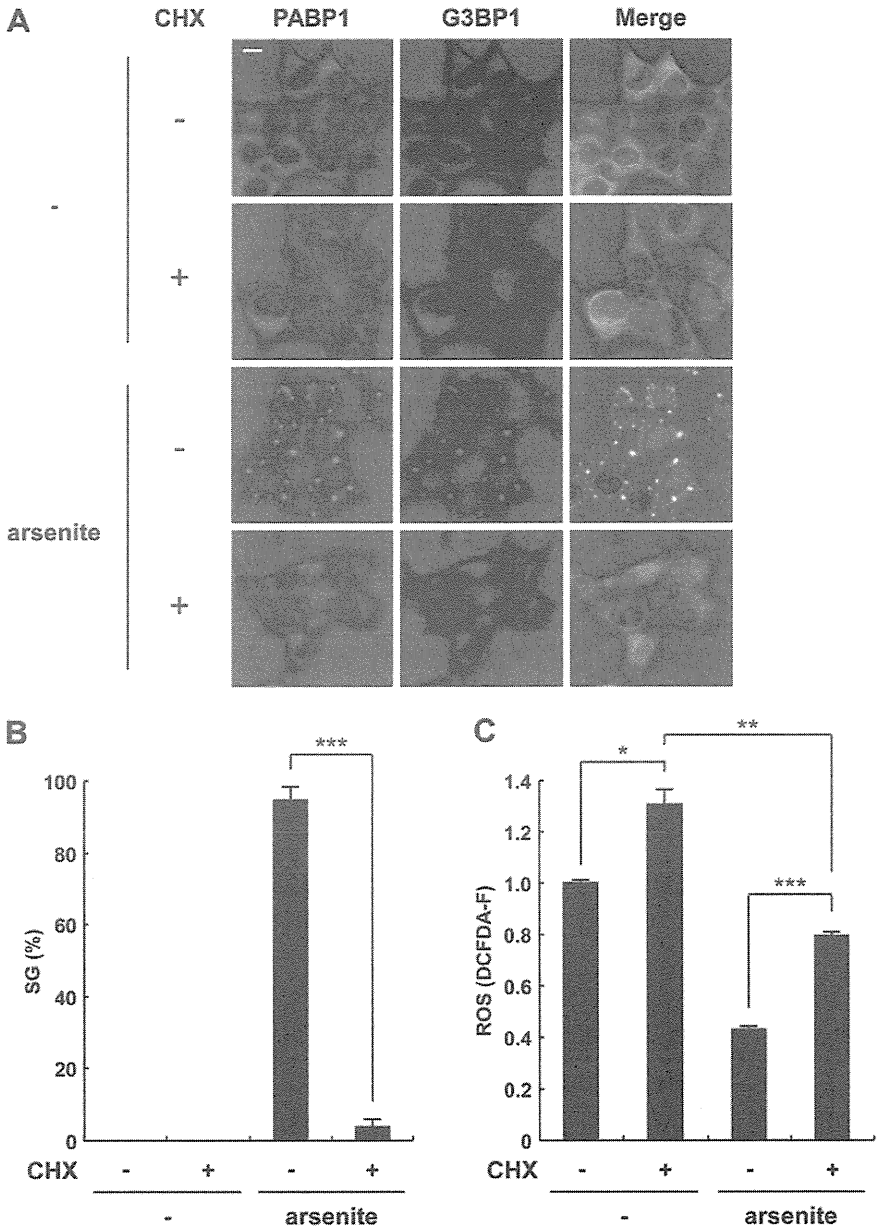

FIG 13 Cycloheximide inhibits SG formation and partially prevents arsenite-induced ROS reduction. (A to C) 293T cells were pretreated with or without 50 μg/ml cycloheximide (CHX) for 30 min, and the cells were further treated with 0.5 mM sodium arsenite for 30 min. The cells were then stained with anti-PABP1 (green) and anti-G3BP1 (red) antibodies and Hoechst 33258 (blue) (A). The bar indicates 10 μm. The SG percentages (B) and the ROS levels (DCFDA-F) (C) are shown. The values denote the means ± SD. *, $P < 0.05$; **, $P < 0.01$; ***, $P < 0.001$.

tions was masked by an excess amount of G3BP1 relative to USP10 in C33A cells.

We then examined the involvement of G3BP1 in ROS-dependent apoptosis. G3BP1 knockdown in C33A cells diminished the ROS level following treatment with arsenite, and the levels were lower than those in the control cells (Fig. 14K). G3BP1 knockdown C33A cells showed less steady-state and arsenite-induced apoptosis than the control cells, and the level of apoptosis was correlated with that of ROS (Fig. 14L). These results suggest that the prooxidant activity of G3BP1 plays a critical role in both steady-state and arsenite-induced apoptosis. These results also suggest that SGs inactivate the prooxidant activity of G3BP1 and that this is part of the mechanism by which SGs reduce the ROS level.

The antioxidant activity of USP10 requires the protein kinase activity of ATM. Ataxia telangiectasia mutated (ATM) protein kinase is oxidated at Cys-2991 by oxidative stressors, such as H_2O_2, and initiates an antioxidant signaling cascade (14). Intriguingly, ATM has been shown to interact with and phosphorylate USP10 (13). To examine the involvement of ATM in USP10-induced ROS reduction, we investigated whether inhibition of ATM protein kinase blocks such USP10 activity. Treatment with KU-

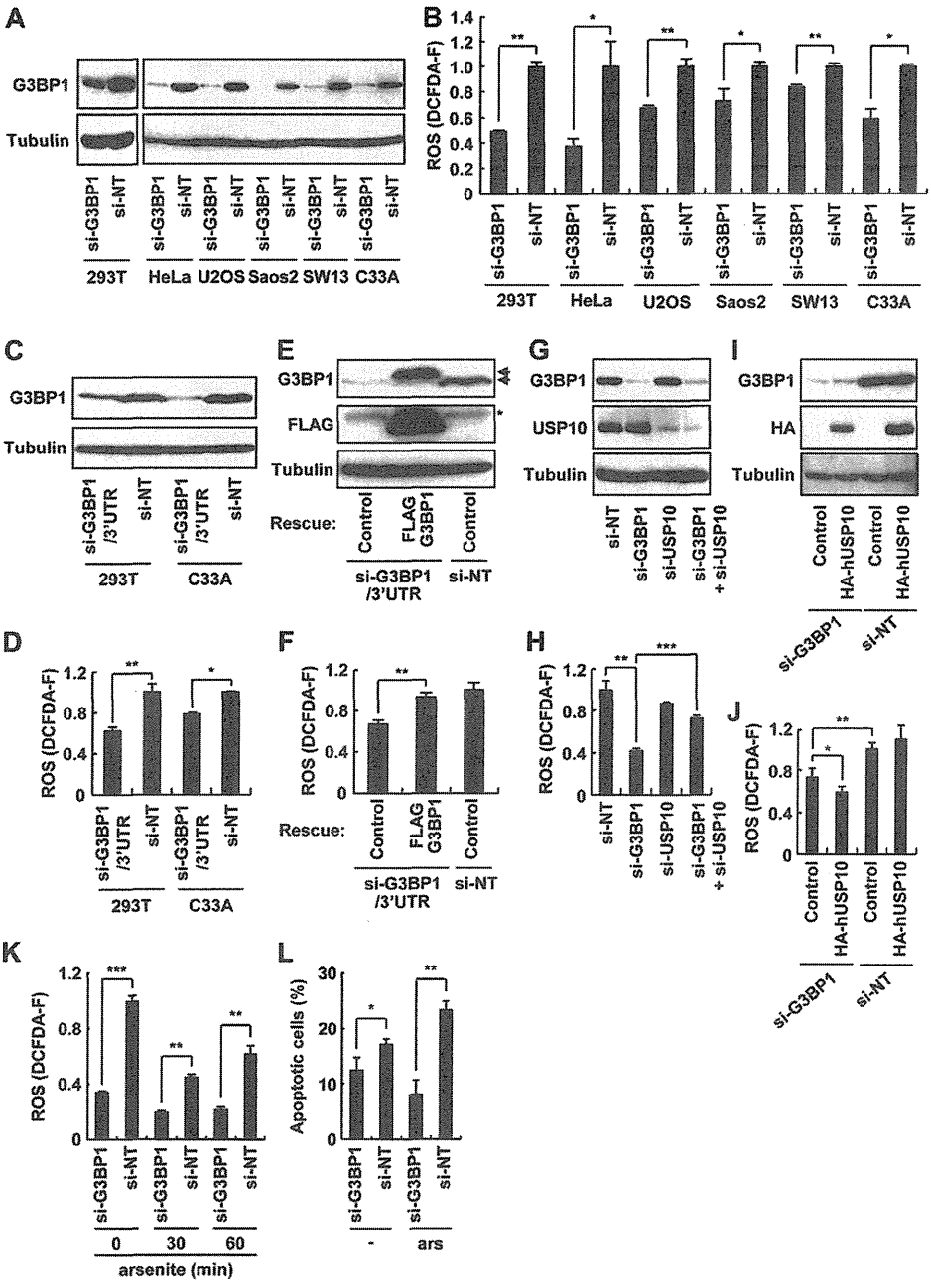

FIG 14 G3BP1 controls steady-state ROS level. (A) The indicated cell lines were transfected with human *G3BP1* siRNA (si-G3BP1) or control nontargeting siRNA (si-NT) for 48 h. The cell lysates prepared from transfected cells were subjected to a Western blot analysis with anti-G3BP1 and anti-α-tubulin antibodies. (B) The cell lines treated in panel A were assessed for ROS production (DCFDA-F). (C and D) 293T and C33A cells were transfected with human *G3BP1* siRNA targeting its 3′ untranslated region (si-G3BP1/3′UTR) or control nontargeting siRNA (si-NT) for 48 h. (C) Cell lysates prepared from transfected cells were subjected to a Western blot analysis with anti-G3BP1 and anti-α-tubulin antibodies. (D) The cells were assessed for ROS production (DCFDA-F). (E and F) 293T cells transfected with the si-G3BP1/3′ UTR or si-NT were further transfected with FLAG-G3BP1 plasmid for 24 h. (E) Cell lysate prepared from transfected cells was subjected to a Western blot analysis with anti-G3BP1, anti-FLAG, and anti-α-tubulin antibodies. The upper and lower arrows indicate exogenous FLAG-G3BP1 and endogenous G3BP1, respectively, and the asterisk indicates a nonspecific band. (F) The cells were assessed for ROS production (DCFDA-F). (G) C33A cells were transfected with si-NT, si-G3BP1, *USP10* siRNA (si-USP10), or si-G3BP1 plus si-USP10 for 48 h, and cell lysates were subjected to a Western blot analysis with anti-G3BP1, anti-USP10-C, and anti-α-tubulin antibodies. (H) Cells treated in panel G were assessed for ROS production (DCFDA-F). (I and J) C33A cells transfected with si-G3BP1 or si-NT were further transfected with plasmids encoding HA-hUSP10 for 24 h. (I) Cell lysates prepared from transfected cells were subjected to a Western blot analysis with anti-G3BP1, anti-HA, and anti-α-tubulin antibodies. (J) The cells were assessed for ROS production (DCFDA-F). (K) C33A cells transfected with the indicated siRNAs were treated with 0.5 mM sodium arsenite for 0, 30, and 60 min, and the cells were assessed for ROS production (DCFDA-F). (L) C33A cells transfected with the indicated siRNAs were treated with 0.5 mM sodium arsenite for 60 min. After being washed, the cells were cultured in fresh medium for 4 h. The cells were then fixed and stained with Hoechst 33258 to detect apoptotic cells. In all panels, the values denote the means ± SD. *, $P < 0.05$; **, $P < 0.01$; ***, $P < 0.001$.

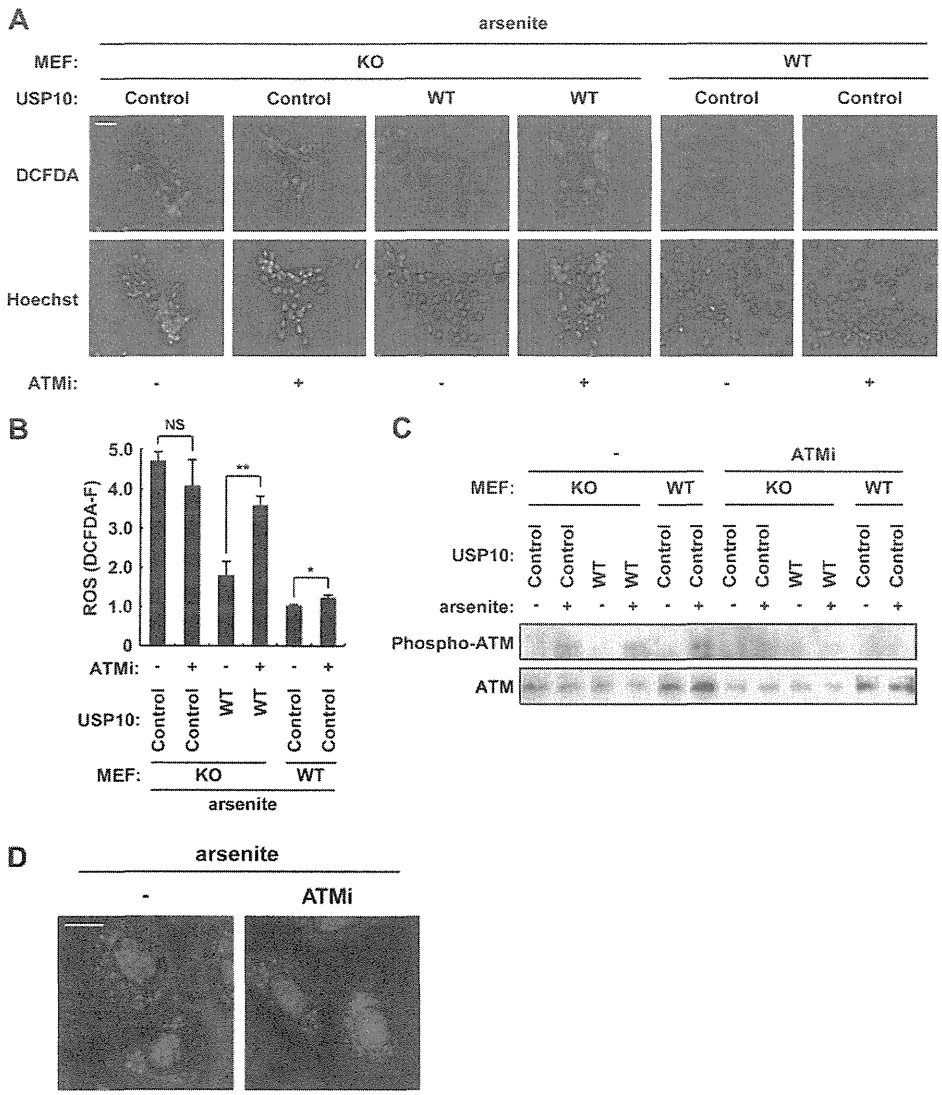

FIG 15 Inhibition of ATM suppresses the antioxidant activity of USP10. (A and B) The indicated MEFs were pretreated with 15 μM KU-55933 (an ATM inhibitor [ATMi]), and the cells were treated with 1 mM sodium arsenite for 100 min and stained with 5 μM CM-H_2DCFDA (green) and Hoechst 33258 (blue) for 5 min at 37°C. The staining was characterized under a fluorescence microscope. The bar indicates 50 μm. The ROS levels (DCFDA-F) in panel A were quantitatively determined using fluorescence analysis software (B). (C) The indicated MEFs were treated with sodium arsenite in the absence and presence of KU-55933, and the cell lysates were characterized using a Western blot analysis with anti-phospho-ATM and anti-ATM antibodies. (D) *USP10*$^{+/+}$ MEFs were treated with sodium arsenite in the absence and presence of KU-55933, and the cells were then stained with anti-PABP1 (green) antibody and Hoechst 33258 (blue). The bar indicates 20 μm. In all panels, the values denote the means ± SD. *, $P < 0.05$; **, $P < 0.01$; NS, not significant.

55933, an ATM inhibitor, upregulated arsenite-induced ROS production in *USP10*$^{+/+}$ MEFs but not in *USP10*$^{\Delta/\Delta}$ MEFs, and the inability to upregulate ROS in the *USP10*$^{\Delta/\Delta}$ MEFs was rescued by the expression of USP10^{WT} (Fig. 15A and B). A Western blot analysis showed that KU-55933 inhibited arsenite-induced ATM phosphorylation at Ser-1981 (Fig. 15C). On the other hand, KU-55993 did not affect SG formation in the 293T cells treated with arsenite (Fig. 15D). Collectively, these results suggest that USP10 is a downstream mediator of the antioxidant signaling of ATM. It is noteworthy that KU-55933 upregulated ROS in the *USP10*$^{\Delta/\Delta}$ MEFs with transduced mUSP10 more significantly than that observed in the *USP10*$^{+/+}$ MEFs (Fig. 15A and B). We assume that ATM downregulates ROS in *USP10*$^{\Delta/\Delta}$ mice exposed to physiological stress, such as hypoxia, and that such a long-term contribution of ATM to ROS regulation in *USP10*$^{\Delta/\Delta}$ mice might therefore enhance the antioxidant role of ATM in *USP10*$^{\Delta/\Delta}$ MEFs.

DISCUSSION

Environmental stressors, such as heat, hypoxia, arsenite, and viral infections, stimulate ROS production. Continuously high ROS production causes tremendously harmful outcomes to cells, organs, and organisms, including DNA damage, massive cell death, inflammation, cancer, and aging (19). To protect against these disasters, cells quickly activate antioxidant mechanisms. We found that SGs have antioxidant activity during these stress responses, and this activity is critical for inhibiting apoptosis and for

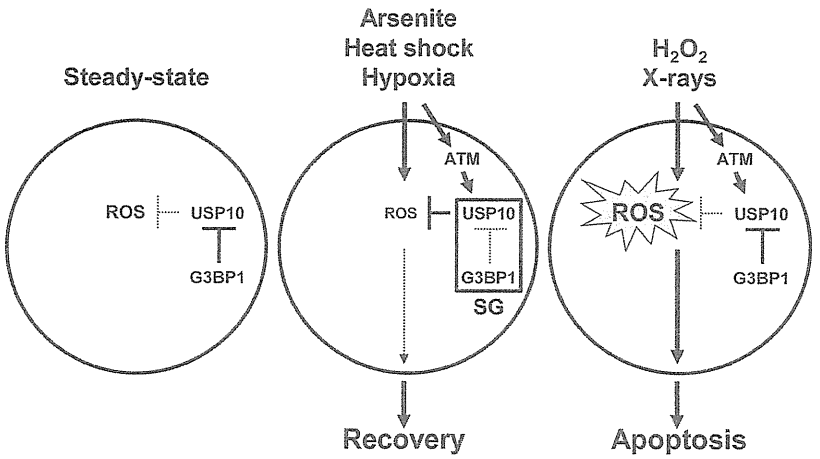

FIG 16 A current model for the functions of SGs, USP10, and G3BP1 in the stress response. G3BP1 masks the antioxidant function of USP10 under steady-state conditions. One type of stress, such as arsenite, heat shock, or hypoxia, induces the formation of SGs and simultaneously activates ATM. SGs inactivate the inhibitory activity of G3BP1 against USP10, and USP10 is activated by ATM or ATM-activated proteins. Next, USP10 reduces ROS production and inhibits ROS-dependent apoptosis. Other types of stress, such as H_2O_2 and X-ray irradiation, do not induce SG formation, and the cells are more prone to undergo apoptosis.

recovery from the stress. This antioxidant activity of SGs is controlled by two SG components, G3BP1 and USP10. USP10 possesses an antioxidant activity; however, the activity observed under steady-state conditions is masked by an excess amount of G3BP1 relative to USP10. However, when cells are exposed to a stress, G3BP1 and USP10 cooperatively induce SGs, and then the SGs, possibly by altering the conformation of USP10 and/or G3BP1, disrupt G3BP1 inhibition against USP10, thereby uncovering the antioxidant activity of USP10 to reduce ROS production (Fig. 16). These findings indicate that SGs are components of a quickly inducible antioxidant machinery that protects cells from detrimental ROS-induced alterations.

The present study detected two distinct antioxidant responses against arsenite: SG-dependent activities and SG-independent activities. SG-independent ROS reduction was detected in the MEFs pretreated with CHX for 30 min after arsenite treatment (early ROS reduction) (Fig. 13). This early ROS reduction was independent of USP10, since it was observed in the *USP10*$^{\Delta/\Delta}$ MEFs (Fig. 8C). The mechanism underlying this early ROS reduction is likely to include the activation of antioxidant enzymes by arsenite, including oxidation of these enzymes, as reported previously (21–23). On the other hand, the SG-dependent antioxidant activity was detected 30 to 100 min after arsenite treatment in MEFs, and the activity was dependent on USP10 (Fig. 8 and 10).

USP10 is a deubiquitinase for p53, and this stabilizes the protein (13). p53 also has an antioxidant activity under various stress conditions (24). However, p53 is not a mediator of USP10 to block ROS production in MEFs treated with arsenite since mUSP10^{C418A}, defective for p53 deubiquitination (13), showed an antioxidant activity equivalent to that of mUSP10^{WT} (Fig. 10), and *USP10*$^{\Delta/\Delta}$ MEFs express p53 protein at a level equivalent to that of *USP10*$^{\Delta/\Delta}$ MEFs expressing mUSP10^{WT} (our unpublished observations).

ATM is activated by various types of oxidative stress stimuli, and accumulating evidence has shown that ATM plays a crucial role in the antioxidant response in a kinase-dependent manner (25, 26). ATM interacts with and phosphorylates human USP10 at Thr-42 and Ser-337; this interaction and phosphorylation are triggered by stress stimuli (13). An ATM inhibitor abrogated the antioxidant activity of USP10 without inhibiting SG formation, thus suggesting that ATM might control the antioxidant activity of USP10 (Fig. 15). It would be interesting, therefore, to clarify whether the USP10 phosphorylation induced by ATM plays a role in the antioxidant activity of USP10. It is unclear how USP10 exerts its antioxidant effect (Fig. 14). USP10 interacts with many proteins localized at polysomes, such as PABPs, HuR, RACK1, and YBX1 (18) (our unpublished observations). Therefore, USP10 might control the stability and/or translation of mRNA(s) involved in redox control; however, the activity might be suppressed by G3BP1 under steady-state conditions.

In summary, our study reveals that USP10 and G3BP1 play critical roles in ROS regulation under both steady-state and stress conditions. Based on our findings, we present a working model for the mechanisms underlying control of ROS and ROS-dependent apoptosis by USP10, G3BP1, and SGs (Fig. 16). The antioxidant function of USP10 is inactivated by G3BP1 under steady-state conditions. Environmental stressors such as arsenite, hypoxia, and heat shock induce the formation of SGs and simultaneously activate ATM. SGs inactivate the inhibitory activity of G3BP1 against USP10, and thus USP10 becomes ready for activation. USP10 is then activated by either ATM-induced phosphorylation or ATM-phosphorylated proteins to reduce ROS and ROS-dependent apoptosis. Other types of stress, such as H_2O_2 and X-ray irradiation, can activate ATM; however, ATM cannot activate USP10 without SGs, and the cells are more prone to undergo apoptosis.

ACKNOWLEDGMENTS

We thank H. Miyoshi (RIKEN Tsukuba Institute, Japan) for lentiviral packaging plasmids and M. Mishina (University of Tokyo, Japan) for *TLCN-Cre* mice. We also thank M. Tobimatsu for technical assistance.

This work was supported in part by a grant-in-aid from the Ministry of Education, Culture, Sports, Science and Technology of Japan and by a grant for the promotion of Niigata University research projects.

REFERENCES

1. Arimoto K, Fukuda H, Imajoh-Ohmi S, Saito H, Takekawa M. 2008. Formation of stress granules inhibits apoptosis by suppressing stress-responsive MAPK pathways. Nat. Cell Biol. 10:1324–1332.
2. Buchan JR, Parker R. 2009. Eukaryotic stress granules: the ins and outs of translation. Mol. Cell 36:932–941.
3. Anderson P, Kedersha N. 2009. RNA granules: post-transcriptional and epigenetic modulators of gene expression. Nat. Rev. Mol. Cell Biol. 10: 430–436.
4. Nover L, Scharf KD, Neumann D. 1989. Cytoplasmic heat shock granules are formed from precursor particles and are associated with a specific set of mRNAs. Mol. Cell. Biol. 9:1298–1308.
5. Tourriere H, Chebli K, Zekri L, Courselaud B, Blanchard JM, Bertrand E, Tazi J. 2003. The RasGAP-associated endoribonuclease G3BP assembles stress granules. J. Cell Biol. 160:823–831.
6. Kedersha NL, Gupta M, Li W, Miller I, Anderson P. 1999. RNA-binding proteins TIA-1 and TIAR link the phosphorylation of eIF-2 alpha to the assembly of mammalian stress granules. J. Cell Biol. 147:1431–1442.
7. Kwon S, Zhang Y, Matthias P. 2007. The deacetylase HDAC6 is a novel critical component of stress granules involved in the stress response. Genes Dev. 21:3381–3394.
8. Solomon S, Xu Y, Wang B, David MD, Schubert P, Kennedy D, Schrader JW. 2007. Distinct structural features of caprin-1 mediate its interaction with G3BP-1 and its induction of phosphorylation of eukaryotic translation initiation factor 2alpha, entry to cytoplasmic stress granules, and selective interaction with a subset of mRNAs. Mol. Cell. Biol. 27:2324–2342.
9. Ortega AD, Willers IM, Sala S, Cuezva JM. 2010. Human G3BP1 interacts with beta-F1-ATPase mRNA and inhibits its translation. J. Cell Sci. 123:2685–2696.
10. Gallouzi IE, Parker F, Chebli K, Maurier F, Labourier E, Barlat I, Capony JP, Tocque B, Tazi J. 1998. A novel phosphorylation-dependent RNase activity of GAP-SH3 binding protein: a potential link between signal transduction and RNA stability. Mol. Cell. Biol. 18:3956–3965.
11. Tourriere H, Gallouzi IE, Chebli K, Capony JP, Mouaikel J, van der Geer P, Tazi J. 2001. RasGAP-associated endoribonuclease G3Bp: selective RNA degradation and phosphorylation-dependent localization. Mol. Cell. Biol. 21:7747–7760.
12. Soncini C, Berdo I, Draetta G. 2001. Ras-GAP SH3 domain binding protein (G3BP) is a modulator of USP10, a novel human ubiquitin specific protease. Oncogene 20:3869–3879.
13. Yuan J, Luo K, Zhang L, Cheville JC, Lou Z. 2010. USP10 regulates p53 localization and stability by deubiquitinating p53. Cell 140:384–396.
14. Guo Z, Deshpande R, Paull TT. 2010. ATM activation in the presence of oxidative stress. Cell Cycle 9:4805–4811.
15. Todaro GJ, Green H. 1963. Quantitative studies of the growth of mouse embryo cells in culture and their development into established lines. J. Cell Biol. 17:299–313.
16. Higuchi M, Tsubata C, Kondo R, Yoshida S, Takahashi M, Oie M, Tanaka Y, Mahieux R, Matsuoka M, Fujii M. 2007. Cooperation of NF-kappaB2/p100 activation and the PDZ domain binding motif signal in human T-cell leukemia virus type 1 (HTLV-1) Tax1 but not HTLV-2 Tax2 is crucial for interleukin-2-independent growth transformation of a T-cell line. J. Virol. 81:11900–11907.
17. Albrecht M, Lengauer T. 2004. Survey on the PABC recognition motif PAM2. Biochem. Biophys. Res. Commun. 316:129–138.
18. Sowa ME, Bennett EJ, Gygi SP, Harper JW. 2009. Defining the human deubiquitinating enzyme interaction landscape. Cell 138:389–403.
19. Thannickal VJ, Fanburg BL. 2000. Reactive oxygen species in cell signaling. Am. J. Physiol. Lung Cell Mol. Physiol. 279:L1005–L1028.
20. Kedersha N, Cho MR, Li W, Yacono PW, Chen S, Gilks N, Golan DE, Anderson P. 2000. Dynamic shuttling of TIA-1 accompanies the recruitment of mRNA to mammalian stress granules. J. Cell Biol. 151:1257–1268.
21. Leiser SF, Miller RA. 2010. Nrf2 signaling, a mechanism for cellular stress resistance in long-lived mice. Mol. Cell. Biol. 30:871–884.
22. Ray PD, Huang BW, Tsuji Y. 2012. Reactive oxygen species (ROS) homeostasis and redox regulation in cellular signaling. Cell Signal. 24: 981–990.
23. Yu R, Chen C, Mo YY, Hebbar V, Owuor ED, Tan TH, Kong AN. 2000. Activation of mitogen-activated protein kinase pathways induces antioxidant response element-mediated gene expression via a Nrf2-dependent mechanism. J. Biol. Chem. 275:39907–39913.
24. Sablina AA, Budanov AV, Ilyinskaya GV, Agapova LS, Kravchenko JE, Chumakov PM. 2005. The antioxidant function of the p53 tumor suppressor. Nat. Med. 11:1306–1313.
25. Alexander A, Cai SL, Kim J, Nanez A, Sahin M, MacLean KH, Inoki K, Guan KL, Shen J, Person MD, Kusewitt D, Mills GB, Kastan MB, Walker CL. 2010. ATM signals to TSC2 in the cytoplasm to regulate mTORC1 in response to ROS. Proc. Natl. Acad. Sci. U. S. A. 107:4153–4158.
26. Cosentino C, Grieco D, Costanzo V. 2011. ATM activates the pentose phosphate pathway promoting anti-oxidant defence and DNA repair. EMBO J. 30:546–555.
27. Matsuki M, Takahashi M, Higuchi M, Makokha GN, Oie M, Fujii M. Both G3BP1 and G3BP2 contribute to stress granule formation. Genes Cells, in press.

Genes to Cells

Both G3BP1 and G3BP2 contribute to stress granule formation

Hideaki Matsuki, Masahiko Takahashi, Masaya Higuchi, Grace N Makokha, Masayasu Oie and Masahiro Fujii*

Division of Virology, Niigata University Graduate School of Medical and Dental Sciences, Niigata 951-8510, Japan

Upon exposure to various environmental stresses such as arsenite, hypoxia, and heat shock, cells inhibit their translation and apoptosis and then repair stress-induced alterations, such as DNA damage and the accumulation of misfolded proteins. These types of stresses induce the formation of cytoplasmic RNA granules called stress granules (SGs). SGs are storage sites for the many mRNAs released from disassembled polysomes under these stress conditions and are essential for the selective translation of stress-inducible genes. Ras-GTPase-activating protein SH3 domain-binding protein 1 (G3BP1) is a component of SGs that initiates the assembly of SGs by forming a multimer. In this study, we examined the role of G3BP2, a close relative of G3BP1, in SG formation. Although single knockdown of either G3BP1 or G3BP2 in 293T cells partially reduced the number of SG-positive cells induced by arsenite, the knockdowns of both genes significantly reduced the number. G3BP2 formed a homo-multimer and a hetero-multimer with G3BP1. Moreover, like G3BP1, the overexpression of G3BP2 induced SGs even without stress stimuli. Collectively, these results suggest that both G3BP1 and G3BP2 play a role in the formation of SGs in various human cells and thereby recovery from these cellular stresses.

Introduction

Upon exposure to various types of stress, such as arsenite, heat shock, hypoxia, and viral infections, mammalian cells activate protective mechanisms to evade the accumulation of DNA and protein alterations. Such protective mechanisms include the formation of stress granules (SGs), which are stress-inducible cytoplasmic granules containing various mRNAs (White *et al.* 2007; Anderson & Kedersha 2009; Buchan & Parker 2009; Holley *et al.* 2011). The formation of SGs is essential for the recovery from stresses and the inability to form SGs induces apoptosis (Kim *et al.* 2005; Arimoto *et al.* 2008).

The formation of SGs is associated with the disruption of polysomes, followed by the transfer of polysome-released mRNAs into SGs in an inactive state (Buchan & Parker 2009). Therefore, one of the main functions of SGs is transient storage of mRNAs during stress. Such storage of mRNAs by SGs is selective, and housekeeping genes are stored in SGs, whereas stress-responsive genes, such as genes encoding heat shock proteins, are able to escape from the storage and are selectively translated to repair stress-induced alterations (Kedersha & Anderson 2002; Stohr *et al.* 2006; Anderson & Kedersha 2009). During the recovery phase, SGs are rapidly dispersed, and the mRNAs stored in SGs have two fates; mRNAs can move back to polysomes to restart translation, or they can move to processing bodies, another type of RNA granule, in which they are degraded (Anderson & Kedersha 2008; Buchan & Parker 2009).

Stress granules contain several RNA-binding proteins, including Ras-GTPase-activating protein SH3 domain-binding protein 1 (G3BP1), TIA-1, eukaryotic initiation factor (eIF)3, eIF4E, eIF4G, poly-A binding protein (PABP), and several ribosomal proteins (rps6, rps3 etc.) (Kedersha *et al.* 1999, 2000; Kedersha & Anderson 2002; Kimball *et al.* 2003; Tourriere *et al.* 2003; Anderson & Kedersha 2006). These RNA-binding proteins are thought to play

Communicated by: Haruhiko Siomi
**Correspondence*: fujiimas@med.niigata-u.ac.jp

DOI: 10.1111/gtc.12023

roles in SG-associated functions. Of them, G3BP1 plays a role in the formation of SGs, as evidenced by the fact that knockdown of G3BP1 reduces the assembly of SGs (Ghisolfi *et al.* 2012). Treatment of cells with arsenite induces the dephosphorylation of G3BP1 at Ser-149, and this dephosphorylation stimulates the multimerization of G3BP1 (Tourriere *et al.* 2003). Therefore, stress-induced multimerization of G3BP1 is likely to initiate SG formation.

The G3BP1 protein can be divided into five regions, the NTF2-like domain, the acidic region, the PXXP motif, and two RNA-binding motifs [an RNA recognition motif (RRM) and an arginine-glycine rich box (RGG)]. The NTF2-like domain and at least one RNA-binding motif are required for SG formation (Tourriere *et al.* 2003). In addition, it has been shown that G3BP1 has an endoribonuclease activity for certain RNAs, although it is unclear whether this activity is associated with functions associated with SGs (Gallouzi *et al.* 1998; Tourriere *et al.* 2001).

G3BP2 is a close relative of G3BP1, with a similar domain architecture, including the NTF2-like domain and two RNA-binding motifs (Kennedy *et al.* 2001; Irvine *et al.* 2004). Like G3BP1, G3BP2 is ubiquitously expressed and is recruited into SGs (French *et al.* 2002; Kobayashi *et al.* 2012). In this study, we examined the role of G3BP2 in the formation of SGs.

Results

G3BP2b is recruited into SGs in various cells

To examine whether G3BP2 is also recruited into SGs, we transfected the FLAG-G3BP2b expression plasmid into HeLa cells, and the cells were then treated with a pro-oxidant, arsenite (Fig. 1). An immunofluorescent analysis showed that FLAG-G3BP2b was mainly localized in the cytoplasm of HeLa cells. Arsenite treatment induced the formation of SGs, as detected by PABP staining in cells, and FLAG-G3BP2b was recruited into these SGs. These results are consistent with the previous study showing that endogenous G3BP2 is recruited into SGs after treatment with arsenite or heat shock (Kobayashi *et al.* 2012).

Both G3BP1 and G3BP2 interact with USP10 and PABP

G3BP1 interacts with ubiquitin specific protease 10 (USP10) and PABP (Soncini *et al.* 2001; Sowa *et al.* 2009), and the interaction of G3BP1 with USP10 is important for the SG-mediated inhibition of apoptosis (manuscript submitted for publication). We therefore examined whether G3BP2 also interacts with USP10 and/or PABP. Cell lysates prepared from 293T cells were immunoprecipitated with anti-G3BP2 antibodies, and the immunoprecipitates were characterized by either anti-USP10 or anti-PABP. Either endogenous G3BP2 or G3BP1 interacted with both endogenous USP10 and PABP (Fig. 2A,B). G3BP1 and G3BP2 have RNA interaction motifs (RRM, RGG in Fig. 3). Therefore, we next examined whether the observed interactions are mediated by RNA bound to G3BPs. The 293T cells were transfected with FLAG-G3BP2b or FLAG-G3BP1 plasmids, and the cell lysates were treated with RNase before undergoing immunoprecipitation. FLAG-G3BP2b and FLAG-G3BP1 interacted with endogenous USP10 and PABP; however, the interactions of G3BPs with PABP but not with USP10 were abrogated by RNase treatment (Fig. 2C). These results indicate that G3BP1 and G3BP2 interact with PABP indirectly through bound RNAs, whereas they interact with USP10 without RNAs.

Next, we examined which domains of G3BP1 and G3BP2b were required for the interaction with USP10 or PABP (Fig. 3). The studies using deletion mutants indicated that the NTF2-like domain of both G3BP1 and G3BP2b is sufficient for their interaction with USP10 (Fig. 3A,C). A further deletion analysis of G3BP1 indicated that the N-terminal 46 amino acids of G3BP1 in the NTF2-like domain are required for the interaction with USP10 (Fig. 3B,D). However, the deletion mutant studies indicated that two regions of G3BP1 and G3BP2b (the NTF2-like domain and the PXXP motif) were independently sufficient for the interaction with PABP.

G3BP1 and G3BP2 double-knockdown impairs SG formation

To elucidate the role of G3BP1 and G3BP2 in SG formation, the amounts of G3BP2 and G3BP1 in cells were transiently reduced by small interfering RNAs (siRNAs) specific for human *G3BP1* or *G3BP2* RNA (G3BP1-siRNA-1, G3BP2-siRNA-1). A Western blot analysis showed that both single and double knockdown significantly reduced the expression of the G3BP2 and/or G3BP1 protein in 293T and HeLa cells (Fig. 4A). To measure the SG formation in these cells, they were treated with 0.5 mM sodium arsenite. Although single knockdown of

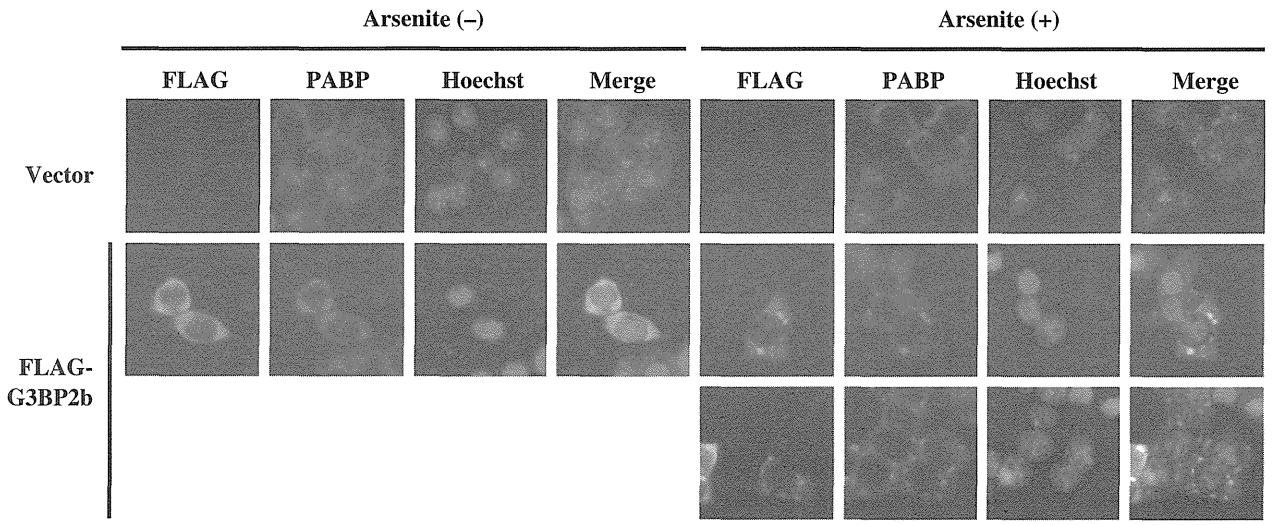

Figure 1 Exogenous G3BP2 is recruited into stress granules (SGs). HeLa cells were transfected with the FLAG-G3BP2b plasmid by a lipofection method using FuGene6. At 48 h after the transfection, cells were treated with sodium arsenite for 60 min. The cells were then stained with anti-FLAG, anti-poly-A binding protein (anti-PABP) and Hoechst33258, and staining was visualized by a fluorescent microscope.

either G3BP1 or G3BP2 partially reduced the number of SG-positive 293T cells, the double knockdown much more significantly reduced the number (Fig. 4B,C). In addition, whereas single knockdown of G3BP2 little affected SG formation in HeLa cells, the knockdown prominently reduced SG formation in G3BP1-knockdown cells. These results indicate that either G3BP1 or G3BP2 is required for arsenite-induced SG formation in 293T and HeLa cells.

To confirm the specificities of the siRNAs used above, we designed a rescue experiment. We first established stable G3BP2-knockdown 293T cells by lentivirus-mediated transduction of *G3BP2* short-hairpin RNA (shRNA) and selection with puromycin. The puromycin-resistant cells were then transiently transfected with G3BP1-siRNA-2, which targets the 3′-untranslated region (UTR) of *G3BP1* RNA. A Western blot analysis confirmed the reduced expression of both G3BP1 and G3BP2 in the double-knockdown cells (Fig. 5A). These double-knockdown cells were then transfected with a FLAG-G3BP1 plasmid, the transcript of which does not have the UTR targeted by the G3BP1-siRNA-2. A Western blot analysis confirmed the expression of wild-type G3BP1 in the FLAG-G3BP1-transfected double-knockdown cells (Fig. 5A). Then, these cells were examined for SG formation (Fig. 5B,C). Exogenous G3BP1 in the double-knockdown cells efficiently rescued the SG formation to a level equivalent to that of wild-type 293T cells. In contrast, the SG formation was not rescued in cells transfected with one of three G3BP1 mutants with a deletion in the NTF2-like domain.

The double-knockdown cells were also transfected with a shRNA-resistant G3BP2b plasmid (Fig. 6). Wild-type G3BP2 protein rescued the SG formation, and the resulting level was equivalent to that in wild-type 293T cells. However, transfection with either of two G3BP2 mutants with a deletion of the NTF2-like domain could not rescue the SG-forming activity (Fig. 6). In addition, neither G3BP1(1–138) nor G3BP2b(1–138) rescued the SG formation, thus indicating that the NTF-like region of G3BP1 or G3BP2 is not sufficient for SG formation (Figs 6, 7). These results indicate that the NTF2-like domain and the rest of the C-terminal region of G3BP2 containing RNA interaction motifs are both required for SG formation. We also noticed that the expression of G3BP2b(139–449), but not G3BP2b(296–449), reduced the number of SG-positive double-knockdown cells (Fig. 6C). This might indicate that the acidic region of G3BP2b has an inhibitory effect on SG formation because there appeared to be an inhibitory effect on the remaining endogenous G3BPs.

Overexpression of G3BP2 without stress induces SG formation

A previous study showed that the overexpression of G3BP1 in cells without stress stimuli induced SG

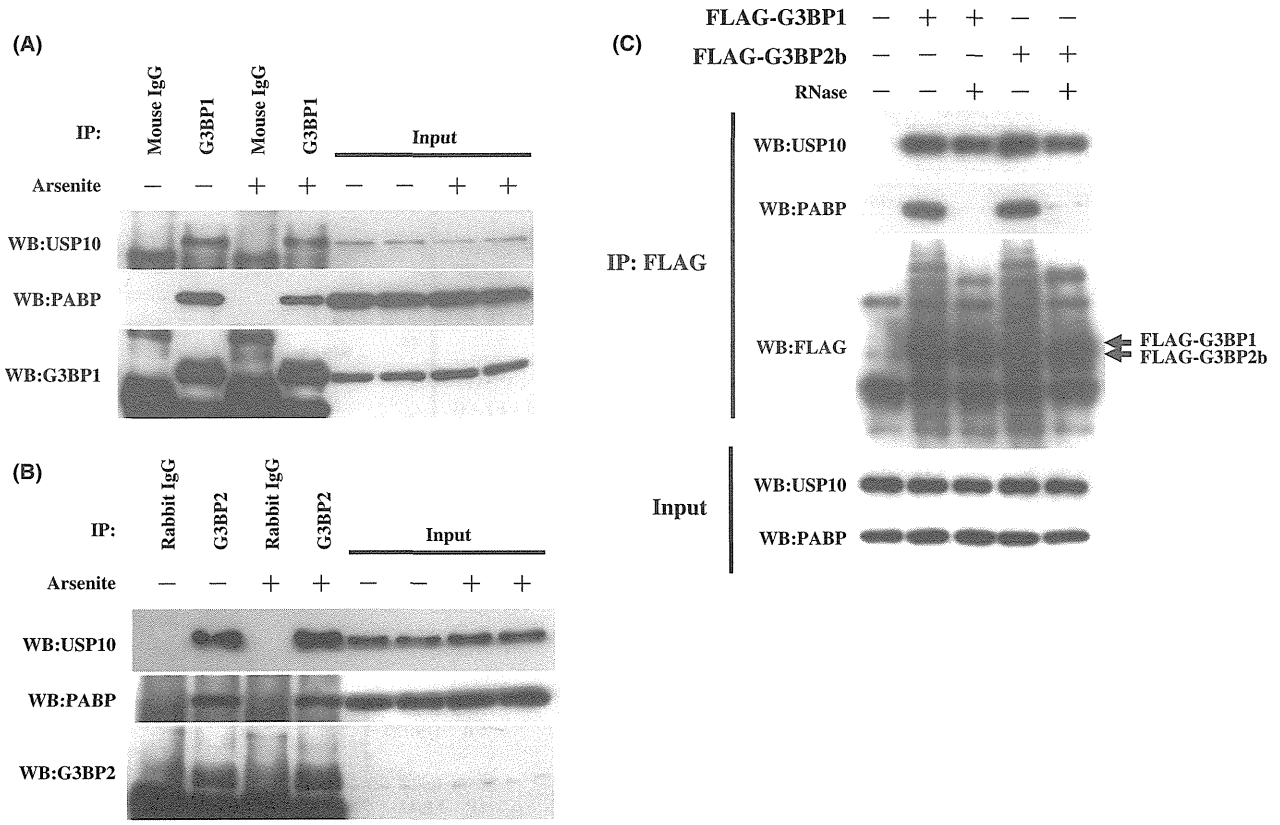

Figure 2 G3BP1 and G3BP2 interact with USP10 and poly-A binding protein (PABP). (A, B) Cell lysates prepared from 293T cells were immunoprecipitated with anti-G3BP1 antibodies (A) or anti-G3BP2 antibodies (B). The cell lysates and immunoprecipitates were then characterized by a Western blotting analysis using anti-USP10, anti-PABP, anti-G3BP1 and anti-G3BP2 antibodies. (C) The 293T cells were transfected with FLAG-G3BP1 or FLAG-G3BP2b using Fugene6. Forty-eight hours after transfection, the cell lysates were prepared and treated with 100 μg/mL RNase for 15 min at 37 °C, and the lysates were then immunoprecipitated with anti-FLAG antibodies. The cell lysates (Input) and immunoprecipitates were characterized by a Western blotting analysis using anti-USP10, anti-PABP, and anti-FLAG antibodies.

formation (Tourriere *et al.* 2003). We therefore examined whether G3BP2 also has a similar activity. The overexpression of G3BP2b in 293T cells also induced SGs, but the number of SG-positive cells (14%) was less than that (27%) of cells overexpressing G3BP1 (Fig. 8). In addition, the size of the SGs induced by G3BP2b was smaller than those induced by G3BP1. These results indicate that G3BP2 by itself has SG-forming activity even in the absence of stress, but its activity is lower than that of G3BP1.

A previous study suggested that the multimerization of G3BP1 after dephosphorylation of Ser-149 is required for SG formation and that the activity is dependent on the NTF2-like domain (Tourriere *et al.* 2003). G3BP2 may also form a multimer, because it also has the Ser-149 adjacent to the NTF2-like domain. To examine this possibility, the 293T cells were transfected with Myc-G3BP2b together with either FLAG-G3BP2b or FLAG-G3BP1, and the cells were treated with arsenite. The cell lysates were then immunoprecipitated with anti-Myc, and the immunoprecipitates were characterized by anti-FLAG antibodies. Myc-G3BP2b immunoprecipitated FLAG-G3BP2b as well as FLAG-G3BP1 before arsenite treatment and the levels were equivalent to those observed after arsenite treatment (Fig. 9A,B). These results suggest that G3BP2 also forms homo- and hetero-multimers with G3BP1 that are likely to be required for SG formation.

Discussion

G3BP1 and G3BP2 have 59% amino acid similarity, and share similar domain structures, including the

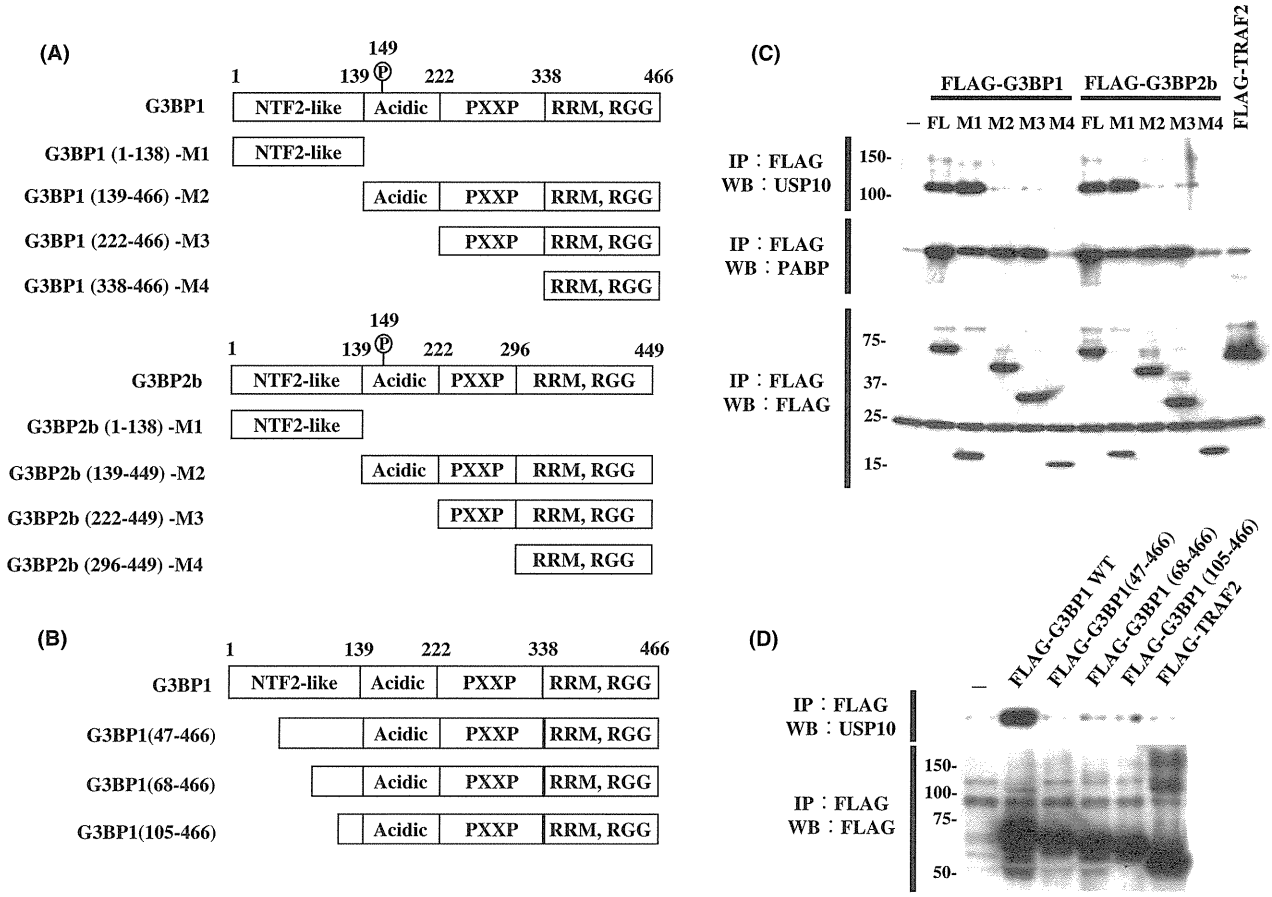

Figure 3 Domains of G3BPs required for interaction with USP10 or poly-A binding protein (PABP). (A, B) Schematic diagrams showing the structures of G3BP1, G3BP2, and their mutants. (C, D) 293T cells were transfected with FLAG-G3BP1, FLAG-G3BP2b or their deletion mutant plasmids using Fugene6. At 48 h after the transfection, cell lysates were prepared and immunoprecipitated with an anti-FLAG antibody. Cell lysates and immunoprecipitates were characterized by a Western blotting analysis using anti-USP10, anti-PABP, and anti-FLAG antibodies.

NTF2-like domain and two RNA-binding motifs (RRM, RGG) (Fig. 3, Kennedy *et al.* 2001; French *et al.* 2002; Irvine *et al.* 2004). We therefore speculated that G3BP2 also plays a role in SG formation. In this study, we showed that G3BP2 is recruited into SGs in 293T and HeLa cells and that either G3BP2 or G3BP1 is required for SG formation induced by arsenite. It should be noted that some tissues studied in mice, such as the brain, muscle and small intestine, dominantly express the G3BP2 protein, whereas G3BP1 was undetectable (Kennedy *et al.* 2001). As a result, in these tissues, G3BP2 might be the main player in SG formation and its associated functions.

G3BP2 formed a homo- and a hetero-multimer with G3BP1 (Fig. 9). Tourriere *et al.* (2003) presented evidence that the augmented multimerization of G3BP1 induced by stress-induced dephosphorylation at Ser-149 initiates SG formation. Collectively, the present study suggests that G3BP1 and G3BP2 form homo- and hetero-multimers to induce SGs. It should be noted that G3BP2 also has the Ser-149 adjacent to the NTF2-like domain and that the amino acid sequences surrounding the Ser-149 of G3BP1 and G3BP2 are highly conserved. Therefore, similar to G3BP1, the dephosphorylations of G3BP2 at Ser-149 induced by stressors might also augment its homo- and hetero-multimerization with G3BP1 to initiate SG formation.

The overexpressions of G3BP2b without stress-induced SG formation in the 293T cells; however, the formation was approximately half of that induced by G3BP1 (Fig. 8). Although the mechanism underlining the difference between G3BP1 and G3BP2 is

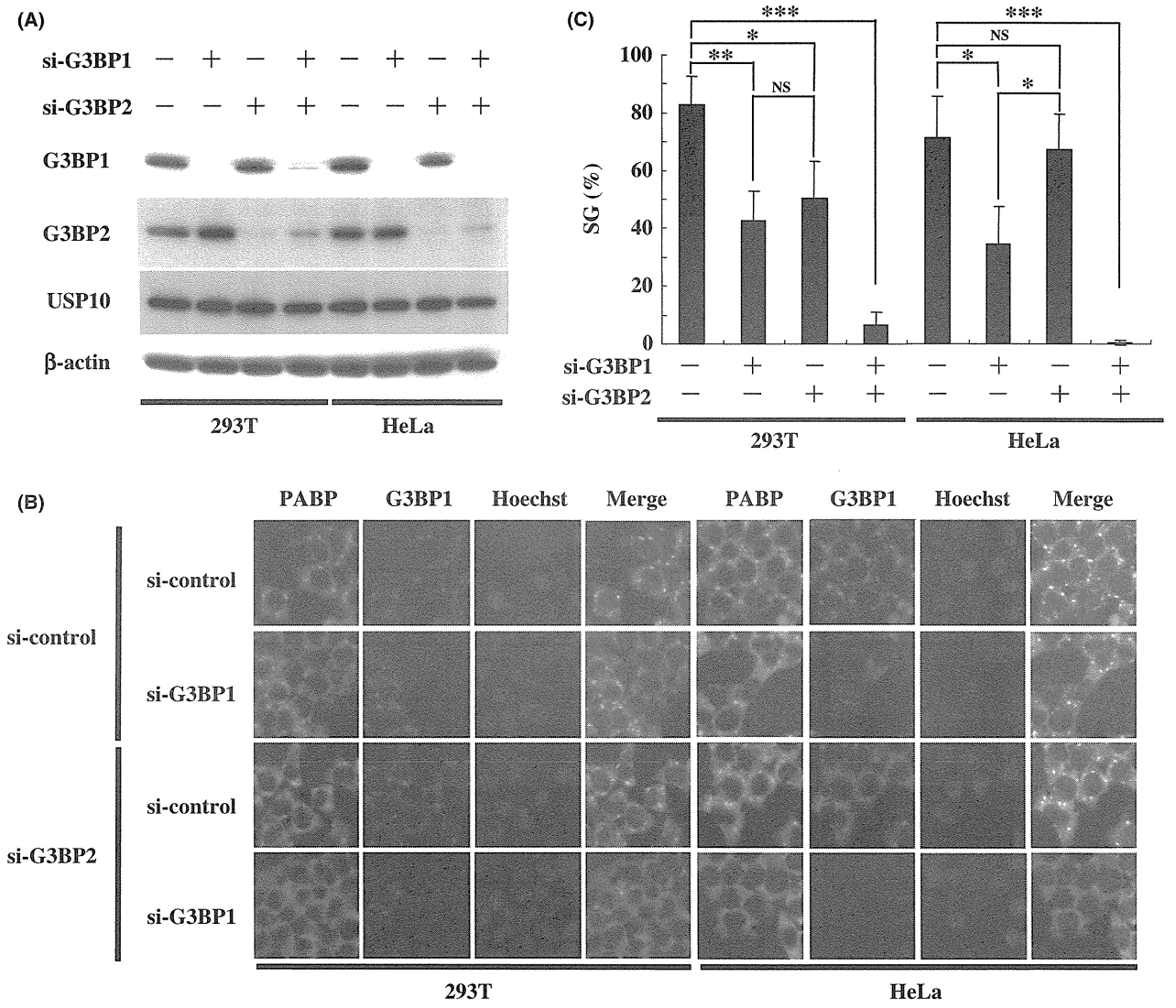

Figure 4 Knockdown of both G3BP1 and G3BP2 reduces stress granule (SG) formation. (A) 293T and HeLa cells were transfected with G3BP1-specific siRNA (G3BP1-siRNA-1) and/or G3BP2-specific siRNA or the control using the Lipofectamine RNAi MAX reagent. At 48 h after the transfection, the cells were characterized by a Western blotting analysis using anti-G3BP1, anti-G3BP2, or anti-β-actin antibodies. (B, C) Cells transfected with the above siRNAs were treated with sodium arsenite for 45 min, and then stained with anti-poly-A binding protein (anti-PABP), anti-G3BP1 and Hoechst33258, and the staining was visualized by a fluorescent microscope (B). The proportion of cells with SGs (%) is presented (C). The data are shown as the means of triplicate experiments and standard deviations. NS, not significant ($P > 0.05$). $*P < 0.05$; $**P < 0.01$; $***P < 0.001$.

unclear at the present moment, the recruitment of RNAs by G3BP2 overexpression might be less than that of G3BP1. Therefore, further analysis is required to determine what causes this difference between G3BP1 and G3BP2 and whether or not the difference has any physiological significance.

The overexpression of the acidic region of G3BP2b without the NTF-like domain reduced SG formation (Fig. 6). A previous study showed that the acidic region of G3BP1 showed inhibitory activity for SG formation (Tourriere *et al.* 2003). Therefore, the acidic region of G3BP1 and G3BP2 might interact with a factor promoting SG formation.

Both G3BP1 and G3BP2 interact with USP10 through the NTF2-like domain. We recently observed that knockout of USP10 in murine embryonic fibroblasts reduces SG formation and augments apoptosis in cells treated with arsenite (submitted for

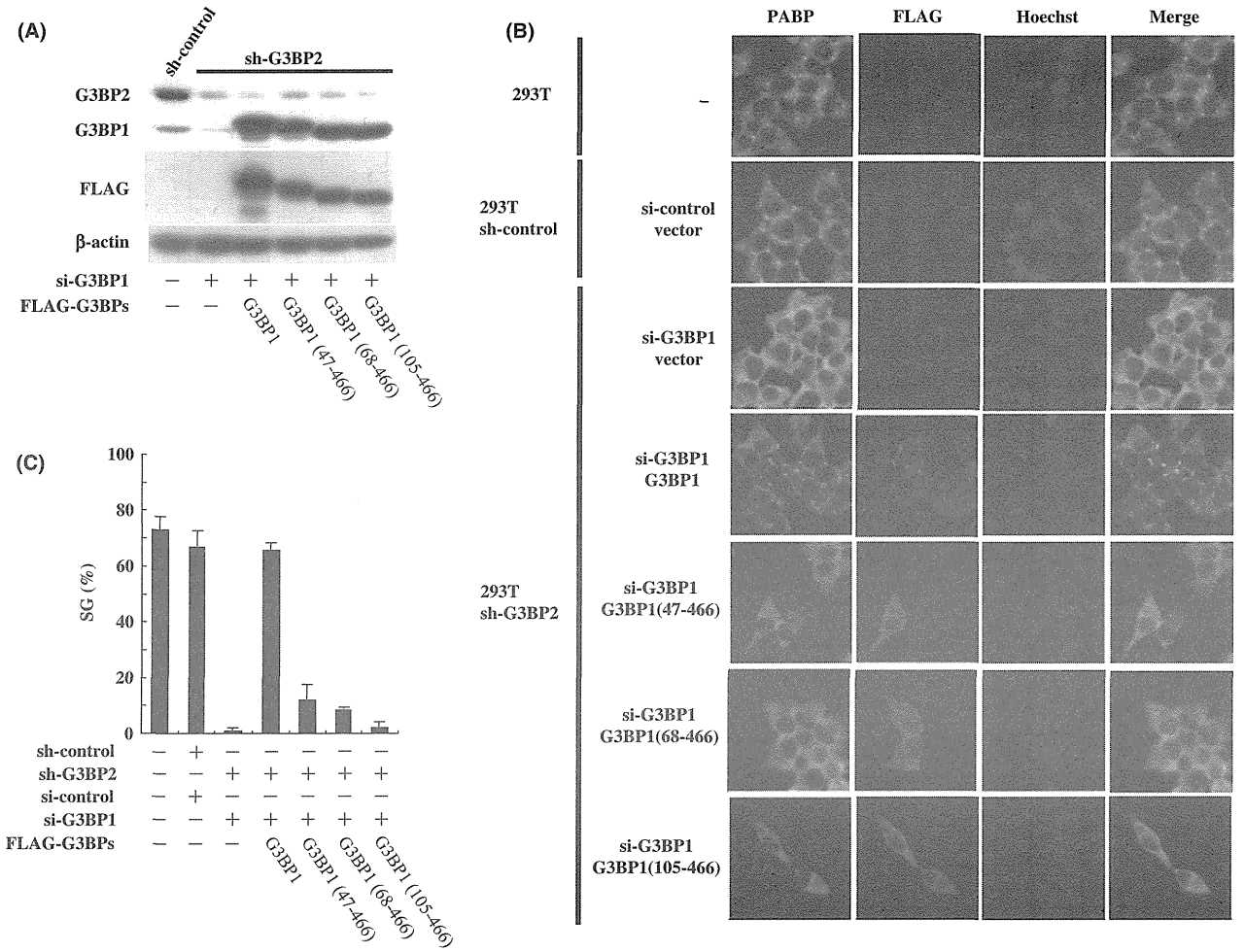

Figure 5 Expression of G3BP1 rescues stress granule (SG) formation. (A–C) G3BP2-knockdown 293T cells and control cells were transfected with G3BP1-siRNA-2 or the control siRNA using Lipofectamine 2000. At 24 h after the transfection, cells were transfected with the FLAG-G3BP1 plasmid or its deletion mutants using Lipofectamine 2000. At 48 h after the transfection, cells were characterized by a Western blotting analysis using anti-G3BP2, anti-G3BP1, anti-FLAG, or anti-β-actin antibodies. (B, C) The indicated cells transfected with siRNAs above were treated with sodium arsenite for 45 min, and then stained with anti-poly-A binding protein (anti-PABP), anti-FLAG and Hoechst33258, and the staining was visualized by a fluorescent microscope. (C) The percentage of cells with SGs (%) is presented. The data are the means of triplicate experiments and standard deviations.

publication). As a result, through its interaction with USP10, G3BP2 might play a role in inhibiting apoptosis under stress conditions. Further studies are required to clearly elucidate the functions of G3BP2 under stress conditions.

Experimental procedures

Cells and culture conditions

The 293T and HeLa cells were originated from human embryonic kidney and human cervical cancer, respectively, and the cells were cultured in Dulbecco's modified Eagle's medium (DMEM) supplemented with 10% heat-inactivated fetal bovine serum (FBS), 4 mM L-glutamine, penicillin (50 μg/mL), and streptomycin (50 μg/mL) at 37 °C in 5% CO_2.

Plasmids

pFLAG-CMV2 is an expression vector encoding a protein with an in-frame FLAG epitope tag at its N-terminus (Sigma-Aldrich). The cDNA fragments of G3BP2b and their mutants were amplified from the pcDNA3.1(+)-G3BP2b plasmid by polymerase chain reaction (PCR), and the frag-

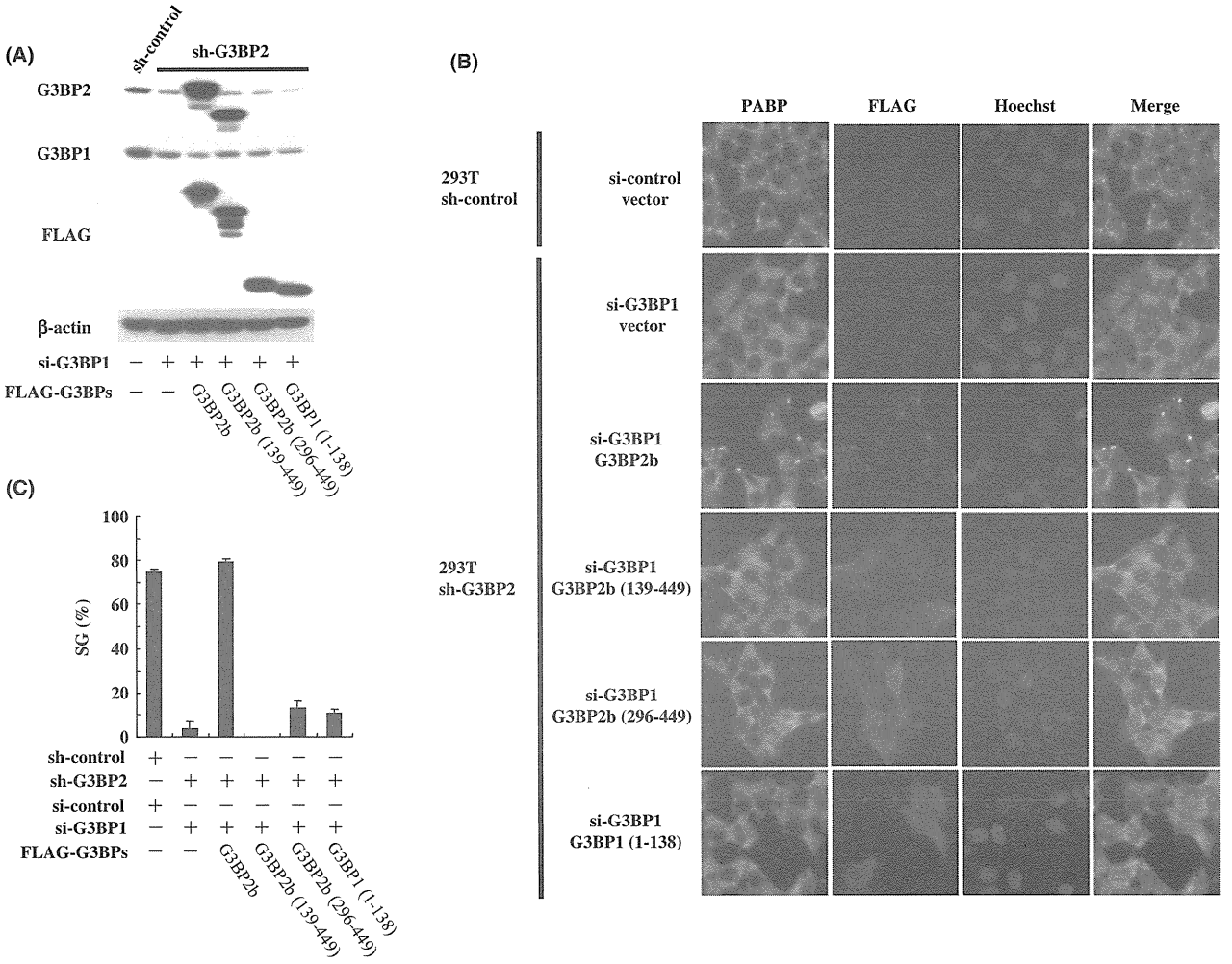

Figure 6 Expression of G3BP2 rescues stress granule (SG) formation. (A–C) G3BP2-knockdown 293T cells and control cells were transfected with G3BP1-siRNA-2 or the control siRNA using Lipofectamine 2000. At 24 h after the transfection, cells were transfected with the FLAG-G3BP2b expression plasmid or its deletion mutants using Lipofectamine 2000. At 48 h after the transfection, cells were characterized by a Western blotting analysis using anti-G3BP2, anti-G3BP1, anti-FLAG, or anti-β-actin antibodies (A). The indicated cells transfected with siRNAs and the plasmids above were treated with sodium arsenite for 45 min, and then stained with anti-poly-A binding protein (anti-PABP), anti-FLAG, and Hoechst33258, and the staining was visualized by a fluorescent microscope (B). The percentage of cells with SGs (%) is presented (C). The data are the means of triplicate experiments and standard deviations.

ments were inserted into the cDNA cloning vector pCR-BluntII-TOPO (Invitrogen) and were then cloned into the *Bgl*II and *Sal*I sites of pFLAG-CMV2. pcDNA6-mycHisA is an expression vector encoding a protein with an in-frame Myc-epitope and 6-histidine-epitope tag at its C-terminus (Invitrogen). The *G3BP2b* cDNA fragment with a deletion of the stop codon was cloned into the *Kpn*I and *Xho*I sites of pcDNA6-mycHisA, and the construct was designated as Myc-G3BP2b. pLKO.1-puro-shG3BP2 expresses a shRNA targeting human *G3BP2* RNA (MISSION shRNA; Sigma-Aldrich). This *G3BP2* shRNA targets both *G3BP2a* and *G3BP2b* RNA.

Small interfering RNAs

The siRNAs specific for human *G3BP1* RNA (Stealth Selected RNAi, siRNA ID: HSS115446) and human *G3BP2* RNA (ID: HSS114988) and negative control siRNAs were purchased from Invitrogen. *G3BP1* siRNA-2 targeting the 3′-untranslated region of human *G3BP1* RNA (ID: SASI_Hs01_00045804) and universal negative control siRNA were purchased from Sigma-Aldrich. Transfection was carried out with 100 pmol siRNAs using Lipofectamine 2000 or Lipofectamine RNAiMAX reagents according to the manufacturer's protocol (Invitrogen).

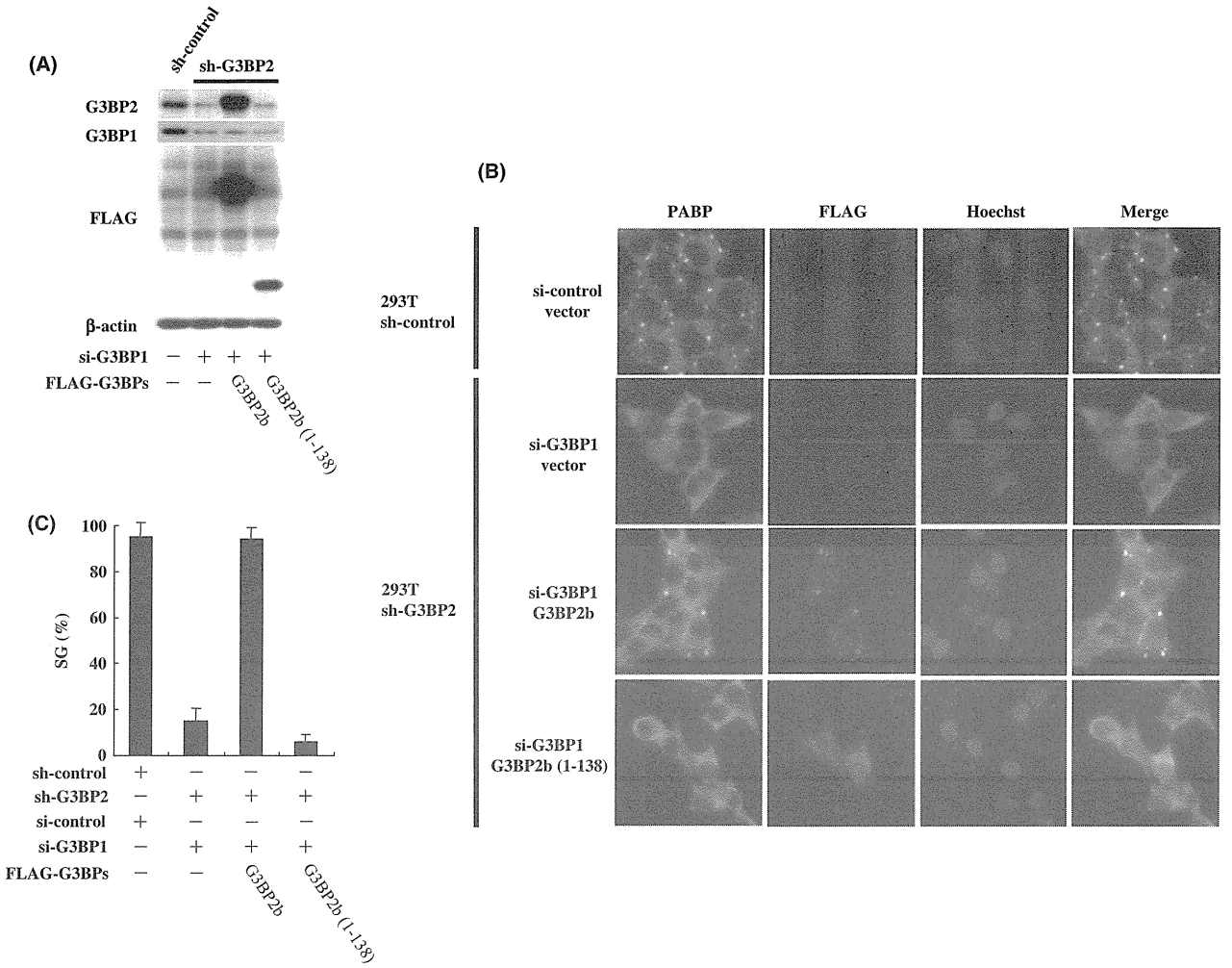

Figure 7 NTF2-like domain of G3BP2 does not rescue stress granule (SG) formation. (A–C) G3BP2-knockdown 293T cells and control cells were transfected with G3BP1-siRNA-2 or the control siRNA using Lipofectamine 2000. Twenty-four hours after transfection, the cells were transfected with FLAG-G3BP2b or FLAG-G3BP2b(1–138) expression plasmids using Lipofectamine 2000. Forty-eight hours after transfection, the cells were characterized by a Western blotting analysis using anti-G3BP2, anti-G3BP1, anti-FLAG, or anti-β-actin antibodies (A). The indicated cells transfected with siRNAs and the above plasmids were treated with sodium arsenite for 45 min and then stained with anti-poly-A binding protein (anti-PABP), anti-FLAG, and Hoechst33258. The staining was visualized using a fluorescent microscope (B). The percentage of cells with SGs (%) is presented (C). The data represent the means and standard deviations of triplicate experiments.

Establishment of G3BP2-knockdown cells

Recombinant lentiviruses were generated by transfecting pCAG-HIVgp, pCMV-VSV-G-RSV-Rev, and pLKO.1-puro-shG3BP2 into 293T cells using FuGENE 6 (Roche). Forty-eight hours after the transfection, the culture supernatant was collected and used to infect 293T cells (2×10^5) in a final volume of 2 mL DMEM/10% FBS containing 8 μg/mL polybrene. At 24 h after the infection, the cells were cultured in the presence of 2 μg/mL of puromycin for 3 days. The expression of the G3BP2 protein in the selected cells was measured by a Western blot analysis.

Short-hairpin RNA-resistant G3BP2b expression vector

The nucleotide sequences of *G3BP2* cDNA targeted by shRNA were mutated by PCR-based site-directed mutagenesis. pFLAG-CMV2-G3BP2b was used as a template for PCR amplification. The nucleotide sequences of the primers were as follows; 5′-CCACAAGGTGTTGTCTCTCAACTTC AGTGAATGTCAT-3′ and 5′-TTCAGAGACAACACCTT-GTGGTGTATATCATTTTGGCC -3′ (the mutated nucleotides were underlined). The mutant *G3BP2b* cDNA fragment was inserted into the pCR-BluntII-TOPO vector, and then

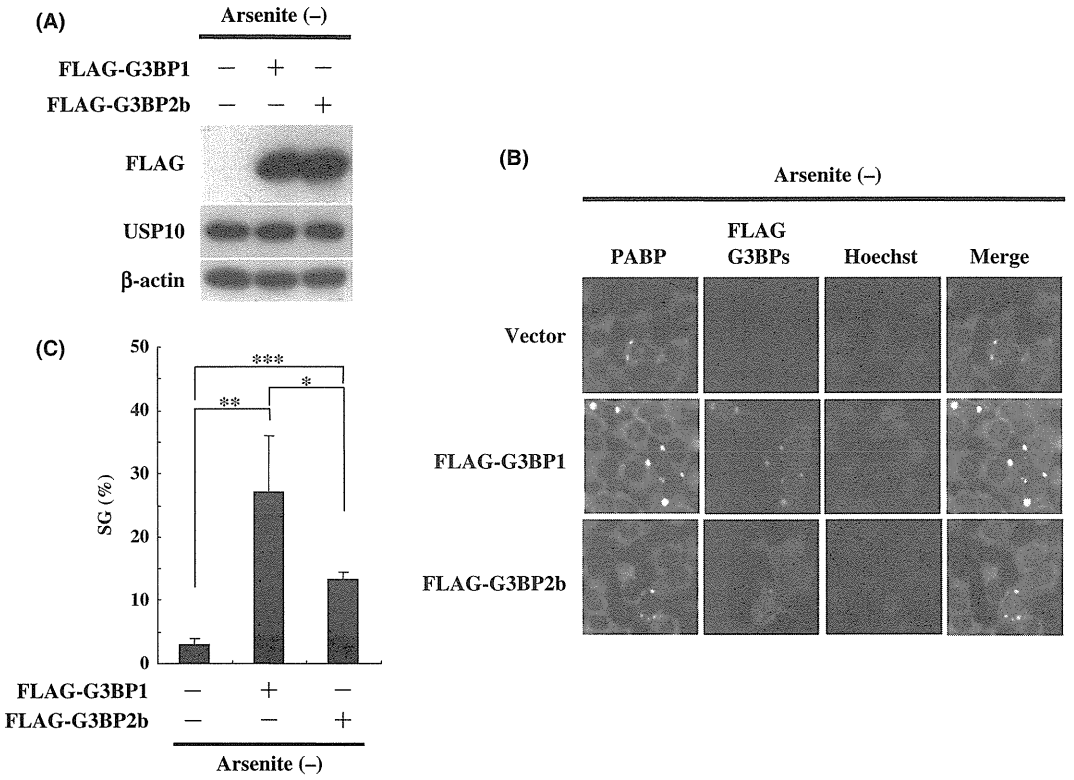

Figure 8 Overexpression of G3BP2 induces stress granules (SGs). (A–C) 293T cells were transfected with the FLAG-G3BP1 or FLAG-G3BP2b plasmid using Fugene6. At 48 h after the transfection, cells were characterized by a Western blotting analysis using anti-FLAG, anti-USP10, and anti-β-actin antibodies (A). At 48 h after the transfection, cells were stained with anti-poly-A binding protein (anti-PABP), anti-FLAG, and Hoechst33258, and the staining was visualized by a fluorescent microscope (B). After examining more than 150 cells, cells with SGs more than 1 μm in size were judged as SG-positive cells, and the proportion of cells with SGs (%) is presented (C). The data are the means of triplicate experiments and standard deviations. $*P < 0.05$; $**P < 0.01$; $***P < 0.001$.

the fragment was inserted into the *Bgl*II and *Eco*NI site of the pFLAG-CMV2 expression vector.

Western blot analysis

Cells were treated with sodium dodecylsulfate (SDS) buffer [2% SDS, 62.5 mM Tris-HCl (pH 6.8), 20% glycerol, 0.01% bromophenol blue, 50 mM dithiothreitol], sonicated, and heated at 95 °C for 5 min. After centrifugation, the supernatants (20 μg) were size-separated on 6–12% polyacrylamide gels containing SDS, and they were then electronically transferred to PVDF membranes. The membranes were incubated with the primary antibody, followed by the corresponding secondary antibody labeled with peroxidase, and the antibody binding was visualized using an ECL Western blotting detection system (GE Healthcare). The primary antibodies used were anti-G3BP1 (BD Bioscience Pharmingen), anti-FLAG (M2 Monoclonal Antibody; Sigma), anti-G3BP2 (Bethyl Laboratories Inc.), anti-USP10 (Bethyl Laboratories Inc.), anti-c-Myc (Sigma), anti-β-actin (Santa Cruz), and mouse anti-α-tubulin monoclonal antibodies (Calbiochem).

Immunostaining analysis and measurement of SG-positive cells

To determine the subcellular localization of PABP, G3BP1, G3BP2, and their mutants, 293T cells were cultured on glass slides on a six-well culture plate for 24 h and then the cells were transfected with G3BP-siRNA (20 nM) or control siRNA using the lipofection method (Lipofectamine 2000). At 24 h after the transfection, the cells were transfected with either the pFLAG-G3BP1 or its deletion mutants using the lipofection method. Twenty-four hours after this transfection, the cells were treated with 0.5 mM sodium arsenite for 60 min. The cells were then washed with PBS and fixed with 4% formaldehyde for 15 min at room temperature. After washing with PBS, the cells were permeabilized with 1% Triton X-100 for 5 min at room temperature, washed with PBS,

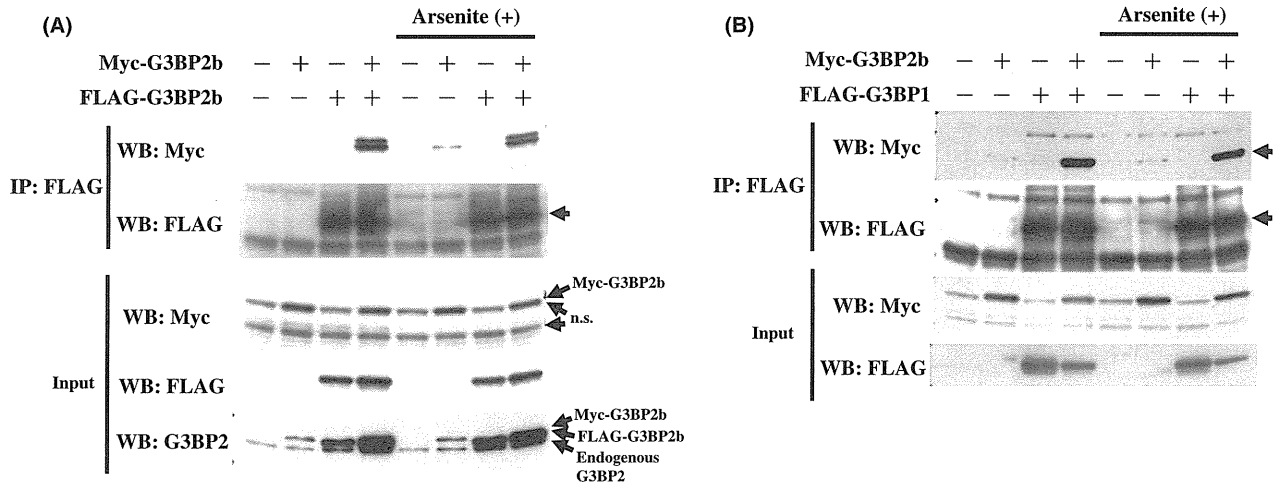

Figure 9 G3BP2 forms a homo- or hetero-multimer with G3BP1. (A, B) 293T cells were transfected with Myc-G3BP2b together with FLAG-G3BP2b plasmids (A) or FLAG-G3BP1 plasmids (B) using Fugene6. Forty-eight hours after transfection, the cells were treated with or without 0.5 mM sodium arsenite for 45 min, then the cell lysates were prepared and immunoprecipitated with anti-FLAG antibodies. The cell lysates (Input) and immunoprecipitates were characterized by a Western blotting analysis using anti-c-Myc, anti-FLAG, anti-G3BP1, and anti-G3BP2 antibodies.

and dried for 20 min at room temperature. The fixed cells were then incubated with 3% bovine serum albumin (blocking solution) for 60 min at room temperature and then the cells were incubated with the primary antibody for 60 min at room temperature. After being washed with 0.2% Triton X-100 three times, the cells were incubated with Alexa594-labeled anti-mouse IgG (Molecular Probes, Eugene, OR, USA), Alexa488-labeled anti-rabbit IgG (Molecular Probes) and Hoechst33258 for 60 min at room temperature. The stained cells were examined by fluorescent microscopy (BZ-8000; KEYENCE). SG formation was examined by anti-PABP staining. After examining more than 150 cells, cells with SGs more than 2 μm in size was judged as SG-positive cells, and the proportion of cells with SGs (%) was calculated. The primary antibodies used were anti-FLAG (M2 monoclonal antibody; Sigma), rabbit anti-FLAG (Sigma), mouse anti-G3BP1 (BD Bioscience Pharmingen), mouse anti-PABP (Sigma), and rabbit anti-PABP (Abcam).

Immunoprecipitation assay

The pFLAG-CMV2-G3BP1, pFLAG-CMV2-G3BP2b plasmids or the deletion mutants (1 μg) were transiently transfected into 293T cells by the lipofection method (Fugene6). At 48 h after the transfection, the cells were treated with lysis buffer (1% Nonidet P-40, 125 mM Tris-HCl, pH 7.2, 150 mM NaCl, 1 mM EDTA, pH 8.0, 1 mM phenylmethylsulfonyl fluoride, 0.2 μg/mL aprotinin) and cell lysates were cleared by centrifugation, and immunoprecipitated with the anti-FLAG antibody. Anti-normal mouse IgG (Santa Cruz) and anti-normal rabbit IgG (Santa Cruz) were used as control antibodies for immunoprecipitation. The immunoprecipitated proteins were characterized by a Western blot analysis using the corresponding primary and secondary antibodies.

Acknowledgements

We would like to thank Dr Masaya Fukushi for providing the pcDNA3.1(+)-G3BP2b, pcDNA3.1-mycHisB and pcDNA6-mycHisA-G3BP2b plasmids. We also wish to thank Dr Hiroyuki Miyoshi at RIKEN Tsukuba Institute for providing the lentivirus plasmids. Finally, we express our gratitude to Misako Tobimatsu for her excellent technical assistance.

References

Anderson, P. & Kedersha, N. (2006) RNA granules. *J. Cell Biol.* **172**, 803–808.

Anderson, P. & Kedersha, N. (2008) Stress granules: the tao of RNA triage. *Trends Biochem. Sci.* **33**, 141–150.

Anderson, P. & Kedersha, N. (2009) RNA granules: post-transcriptional and epigenetic modulators of gene expression. *Nat. Rev. Mol. Cell Biol.* **10**, 430–436.

Arimoto, K., Fukuda, H., Imajoh-Ohmi, S., Saito, H. & Takekawa, M. (2008) Formation of stress granules inhibits apoptosis by suppressing stress-responsive MAPK pathways. *Nat. Cell Biol.* **10**, 1324–1332.

Buchan, J.R. & Parker, R. (2009) Eukaryotic stress granules: the ins and outs of translation. *Mol. Cell* **36**, 932–941.

French, J., Stirling, R., Walsh, M. & Kennedy, H.D. (2002) The expression of Ras–GTPase activating protein SH3 domain-binding proteins, G3BPs, in human breast cancers. *Histochem. J.* **34**, 223–231.